Theory of mean E×B shear in a stochastic magnetic field: ambipolarity breaking and radial current

To cite this article before publication: Weixin Guo *et al* 2022 *Plasma Phys. Control. Fusion* in press https://doi.org/10.1088/1361-6587/ac93b0

Theory of mean E×B shear in a stochastic magnetic field: ambipolarity breaking and radial current

Weixin Guo[1, *], Min Jiang[2, *], Patrick H. Diamond[2, 3, **], Chang-chun Chen[3], Mingyun Cao[3], Hanhui Li[1] and Ting Long[2]

[1]International Joint Research Laboratory of Magnetic Confinement Fusion and Plasma Physics, State Key Laboratory of Advanced Electromagnetic Engineering and Technology, School of Electric and Electronic Engineering, Huazhong University of Science and Technology, Wuhan 430074, China

[2]Center for Fusion Science, Southwestern Institute of Physics, P. O. Box 432, Chengdu, Sichuan 610041, China.

[3]Center for Astrophysics and Space Sciences, University of California San Diego, La Jolla, California 92093, USA.

E-mail: pdiamond@ucsd.edu, wxguo@hust.edu.cn

Abstract

The mean **E×B** shear in a stochastic magnetic field is calculated, using the radial force balance relation and transport equations. This analysis is relevant to the L→H transition with resonant magnetic perturbations (RMP), and special focus is placed upon the physics of non-ambipolar transport and radial current. The key physical process is the flow of fluctuating current along wandering magnetic fields. The increments in poloidal and toroidal rotation, density and ion pressure are calculated. The radial envelope of the magnetic perturbations inside the plasma defines a new scale ℓ_{env}, which is the characteristic scale of the magnetic fluctuation intensity profile. The net particle outflow due to stochastic magnetic fields is calculated and is determined by the net radial current through the separatrix. Implications for the L→H transition are discussed.

Key words: E×B shear, stochastic magnetic field, ambipolarity breaking, radial

*Joint first authors.

**Author to whom any correspondence should be addressed.

current, L-H transition

1. Introduction

The discovery of the low confinement to high confinement (L→H) transition more than 40 years ago [1] continues to have a major impact on the magnetic fusion program and, more broadly, the science of plasmas physics. The high confinement mode (H-mode) saved magnetic fusion energy (MFE) from the pessimism of Goldston scaling [2], and introduced transport barriers and bifurcations, -or, equivalently-, realized the concepts of confinement "phases" and transitions [3]. The H-mode focused attention on the role of the flow profile, especially the flow shear, in confinement. As understanding of transport bifurcations improved, attention shifted to dynamical feedback loops, thus leading to models of the predator-prey system type [4]. These also are characteristic of drift wave-zonal flow systems in magnetic fusion devices. The H-mode also forced us to address the consequences of a marked reduction in transport, and so the need for transport regulation. Indeed, in the present day, attention has shifted to *control* of the H-mode, so as to optimize the interplay of core and edge transport [5].

The $\mathbf{E}\times\mathbf{B}$ flow profile [6], especially its shear and curvature, is undoubtedly a key element of the L to H transition. Virtually, all L→H transition models in some way exploit the feedback of mean $\mathbf{E}\times\mathbf{B}$ shear on turbulence, though the trigger mechanisms proposed (i.e., Reynolds stress, orbit loss etc.) may differ. $\mathbf{E}\times\mathbf{B}$ shear enhanced decorrelation is a robust and physically appealing mechanism for turbulence suppression. Thus, it is essential to have a good understanding and model of $\mathbf{E}\times\mathbf{B}$ shear, in order to confront the complexities of the L→H transition.

As the H-mode becomes the preferred regime of enhanced confinement, awareness grows of the need to reconcile good power handling with good confinement. In practice, good power handling requires boundary and heat load control, and these naturally require some ways to suppress or mitigate giant edge localized modes (ELM) [7]. These considerations drive the development of the resonant magnetic perturbations (RMP), which mitigate ELM by inducing a thin stochastic layer at the plasma boundary [8].

One may note that the changes in magnetic topology induced by RMP are similar to what follows the application of the lower hybrid waves (LHW), where helical current filaments aligned with magnetic field lines are observed in the scrape-off layer (SOL) [9, 10]. Recent experiments on EAST found that the response of ELM (i.e., suppression/mitigation or triggering) to LHW modulation depends upon the LHW coupling to the plasma and the effect of the LHW on the pedestal density profiles [11-13]. In this paper, we put our focus on plasmas with RMP, where edge turbulence co-exists with this stochastic layer [14] produced by three-dimensional (3D) magnetic perturbations (MP). Stochastic fields occur when the separation of magnetic field lines grows exponentially (i.e., there exists one positive Lyapunov exponent). In practice, magnetic island overlap is a good working criterion for stochasticity. The degree of stochastization can be quantified by the ratio of the auto-correlation length to the scattering length l_{ac}/l_c ($l_{ac} = 1/|\Delta k_{\parallel}|$ and $1/l_c = \left(\frac{k_\theta^2 D_M}{3L_s^2}\right)^{1/3}$ [15, 16], where $D_M = \sum_{\boldsymbol{k}} |\tilde{b}^2_{r,\boldsymbol{k}}| \pi\delta(k_{\parallel})$ is the stochastic magnetic diffusivity, $k_{\parallel}$ and k_θ are parallel and poloidal wavenumber, respectively, and L_s is scale length of magnetic shear). The ratio l_{ac}/l_c is related to the Kubo number [17].

It is well known that both the parallel and perpendicular transport are important in determining the transport across an island or stochastic region. This follows from the viewpoint of both classical collisional theory and micro-turbulence [18-23]. In the literature, Rosenbluth et al [24] described such destruction of magnetic surfaces by magnetic field irregularities, and Rechester and Rosenbluth [19] studied the electron heat transport due to destroyed magnetic surfaces. Meanwhile, many magnetic-stochasticity-based theoretical models have been developed [25-30], and the increase of plasma transport at the edge due to the application of RMP has been reported. Operation with RMP then encountered the challenge of making the L→H transition in the presence of a pre-existing, thin stochastic layer at the boundary. One may be tempted to doubt the role of this thin stochastic layer, but it is indeed located precisely where the L-H transition is triggered, on the outboard midplane separatrix in DIII-D [14]. Note that edge turbulence and flows evolve in this stochastic layer. The physics of the

transition thus becomes conflated with the physics of RMP pump-out and Reynold stress decoherence [8, 30, 31]. An increase in the power threshold for L→H transition due to the application of RMP has been reported on multiple devices. This is summarized later. All of these phenomena added new challenges to the understanding of the L→H transition. Thus, it is of prime importance to understand the physics of **E×B** shear layer structure in a stochastic magnetic field. A theory of the mean $\langle E_r \rangle$ in such an environment clearly is essential to develop such an understanding. Hence, we deem it appropriate for the Special Issue, as a contribution on an aspect of L→H physics of present day and future (i.e., ITER and CFETR, etc.) interest.

Here, we briefly summarize the impact of the MP field with different toroidal mode numbers (n) on the L-H transition power threshold (P_{LH}). This has been comprehensively investigated in multiple existing fusion devices such as DIII-D with n=3 [14, 32, 33], NSTX with n=3 [34], ASDEX-Upgrade with n=2 [35-37], MAST with n=2, 3, 4, 6 [38, 39], JFT-2M with n=1, 2, 3, 4, 6 [40] and KSTAR with n=1 [41, 42]. A significant increase in the P_{LH} is found when RMP is applied, but little effect is noted for non-resonant MP fields [14, 32, 33]. Edge layer stochastization due to RMP appears to be fundamental. A clear threshold in $\delta B_r/B_T$ strength for the increase of P_{LH} by RMP [14, 32, 36-38, 41, 42] has been observed. For DIII-D with an n=3 field, this threshold is smaller than the minimum strength requirement for ELM suppression. This inequality suggests a concern for ITER H-mode access, especially in the pre-Fusion power operation (PFPO) phase, where the available heating power is marginal [14, 32]. However, in ASDEX-Upgrade with n=2 field, the critical $\delta B_r/B_T$ for P_{LH} increases and is above that for ELM suppression. This may open a window of the MP strength for ELM suppression without any increase in P_{LH}. Of course, the required power for ELM suppression can also be sensitive to penetration and plasma response [43]. An explanation for how the RMP raises the power threshold likely is related to the edge stochasticity and a resonant electro-magnetic torque, which causes a reduction of the **E×B** flow shear [14, 33, 37, 38]. These lead to an increase in the turbulent transport [14, 33], and a reduction of the Reynold stress driven poloidal flow [33]. For the latter,

decoherence must occur. Nevertheless, the interactions among the plasma profiles, flows and turbulence preceding the L-H transition with MP application are not clear [44]. Hence, it is difficult to establish a multi-machine database. Relevant insight from theoretical study is needed. This paper aims to supply the relevant physical insights.

In this paper, we present a mean field theory for **E**×**B** shear in an ambient stochastic layer, such as may be found at the edge of an RMP plasma. A novel way to approach this analysis is to revisit the expression for radial electric field $\langle E_r \rangle$ as given by the ion radial force balance equation,

$$\langle E_r \rangle = \frac{\langle \nabla P_i \rangle}{e n_i} - \langle V_\theta \rangle B_\phi + \langle V_\phi \rangle B_\theta .$$

Here, ∇P_i means the ion pressure gradient, e is the elementary charge and n_i is ion density, V_θ and V_ϕ are poloidal and toroidal velocity, B_ϕ and B_θ are toroidal and poloidal magnetic fields, respectively. Thus, the impact of stochasticity on $\langle E_r \rangle$ must arise via changes in $\langle V_\theta \rangle$, $\langle V_\phi \rangle$, $\nabla \langle P_i \rangle$ and $\langle n_i \rangle$. *These all are modified by the mean radial current density* $\langle J_r \rangle$*, which is induced by the correlation of radial magnetic perturbations* $\tilde{b}_r = \tilde{B}_r / B_0$ *with parallel current fluctuations* $\tilde{J}_\parallel$*, as* $\langle J_r \rangle = \langle \tilde{J}_\parallel \tilde{b}_r \rangle$. Here, $\tilde{b}_r$ and $\tilde{J}_\parallel$ in the plasmas are necessarily linked by Ampere's law, even if external perturbations are used to generate $\tilde{b}_r$. Radial current density directly changes the various components of the radial force balance expression according to the following three points: (1) $\langle V_\theta \rangle$ is driven by $\langle J_r \rangle B_\phi$; (2) $\langle V_\phi \rangle$ is driven by $\langle J_r \rangle B_\theta$; (3) n_i will be evolved by $\frac{\partial \langle J_r \rangle}{\partial r}$, via the continuity equation. In the following, we assume a pure, hydrogenic plasma, thus the densities of ions and electrons, which adjust due to the radial electric field are the same, and we will not distinguish them, i.e., $n_i = n_e = n_0$. Besides, all the above, the ion temperature T_i is also necessarily modified by the stochastic magnetic fields, though an explicit and direct connection to radial current density is not apparent. *Thus, the radial current density emerges as the key indicator of "non-ambipolar transport" induced by magnetic stochasticity.* The challenge then is to

calculate $\langle J_r \rangle$.

We calculate the mean radial current density by exploiting Ampere's law and using the fact that ion flow contributes to $\langle J_{r,e} \rangle$. The latter piece is important, as toroidal rotation enters via the total mean radial current density $\langle J_r \rangle$. A significant toroidal rotation velocity is usually necessary to avoid locked modes in RMP plasmas [45-47]. We show that current density necessarily depends upon the divergence of the magnetic stress. This, in turn, varies rapidly across the thin stochastic layer. The magnetic stress also depends on the cross phase factor between $\tilde{b}_r$ and the perturbed poloidal field $\tilde{b}_\theta$. Approaching the L→H transition, the phase is set by the mode structure, evolving radial electric field shear and the eddy tilting it induces. Radial current density directly enters the evolution of $\langle V_\theta \rangle$, $\langle V_\phi \rangle$ and $\langle n_e \rangle$ (here, $\langle n_i \rangle = \langle n_e \rangle$), and so modifies all of them. As mentioned earlier, magnetic perturbations enter the evolution of mean ion temperature $\langle T_i \rangle$, albeit weakly. These all are calculated, and a novel mean field model for $\langle E_r \rangle$ is developed. The $\langle E_r \rangle$ model can be used to extend a multi-field model of L→H transition to include the effects of non-ambipolar transport contributions due to the stochasticity. The implications for L→H transition evolution are discussed. Note that in contrast to previous works on this subject, no apriori quasi-linear (or "test particle") approximations are made. We will discuss more about this in the next section.

The reminder of this paper is organized as follows. Section 2 contains the calculation of the mean radial current density $\langle J_r \rangle$ induced in a stochastic layer. In section 3, evolution equations for $\langle V_\theta \rangle$, $\langle V_\phi \rangle$ including effects of $\langle J_r \rangle$ are derived. Flows are calculated in some simple limits. Section 4 derives the evolution of density and temperature with $\langle J_r \rangle$. In Section 5, we discuss the direct effects of the ambient stochasticity on the pre-transition turbulence. The transition model is discussed in Section 6. The novel contributions to $\langle E_r \rangle$ from magnetic stochasticity are parsed, and their implications for L→H transition models are discussed. Section 7 presents conclusions and an outline of future plans.

2. Mean radial current density

In this section, we calculate the mean radial current density $\langle J_r \rangle$ and mean radial electron current density $\langle J_{r,\mathrm{e}} \rangle$ produced by a stochastic magnetic field. $\langle J_r \rangle$ contains the non-ambipolar transport, and enters the net effect on charge balance. $\langle J_r \rangle$, the total radial current density, enters mean radial electric field shear via $\langle V_\theta \rangle$ and $\langle V_\phi \rangle$. The mean radial electron current enters via evolution of electron density (and the condition of $\langle n_i \rangle = \langle n_e \rangle$). The two radial current densities represent the principal non-ambipolar effects induced by the stochastic magnetic field.

A short discussion of the concepts of ambipolarity and ambipolarity breaking is in order here. A transport process which maintains exact local charge balance is said to be ambipolar. Non-ambipolar processes result from a deviation from local balance. Examples include:

— a flux of polarization charge $\langle \tilde{V}_r \tilde{\rho}_{pol} \rangle$ which preferentially transports ions relative to electrons. Here, $\tilde{V}_r$ is the fluctuating radial velocity, and $\tilde{\rho}_{pol}$ is the polarization charge density fluctuation. Recall that the ion inertia and thus the scale of the polarization drift greatly exceeds its electron counterpart, so $\langle \tilde{V}_r \tilde{\rho}_{pol} \rangle$ is mainly carried by ions;

— a radial current density due to current flow along the wandering magnetic field lines, i.e., $\langle \tilde{b}_r \tilde{J}_\parallel \rangle$. This process preferentially transports electrons.

Both polarization flux and current flow along the wandering magnetic field lines can break ambipolarity and so influence the mean electric field $\langle E_r \rangle$. Note that a flux may be non-ambipolar yet still respect quasi-neutrality, by allowing local deviation from charge balance while maintaining $n_i = n_e$ -and thus charge balance- on the scale of the fluctuation envelope. Observe that a multiscale framework is required to address questions of ambipolarity breaking in turbulent transport. In particular, we identify two relevant radial scales of the turbulence as shown in figure 1:

— Δ_c, the characteristic radial correlation scale of fluctuations (i.e., mode width);

— ℓ_{env}, the radial envelope or spectral scale, which is characteristic scale of the fluctuation intensity profile.

In principle, each of the electrostatic fluctuations and stochastic perturbations will support Δ_c and ℓ_{env}. Note that for electrostatic fluctuations, Δ_c is set by drift wave propagation physics, while ℓ_{env} is set by absorption (i.e., ion Landau damping). For the magnetics, diamagnetic coupling effects related to drift wave coupling and propagation will generate Δ_c. As the stochastic layer in figure 2 from DIII-D is narrow [14], ℓ_{env} will necessarily be small (around a few centimeters).

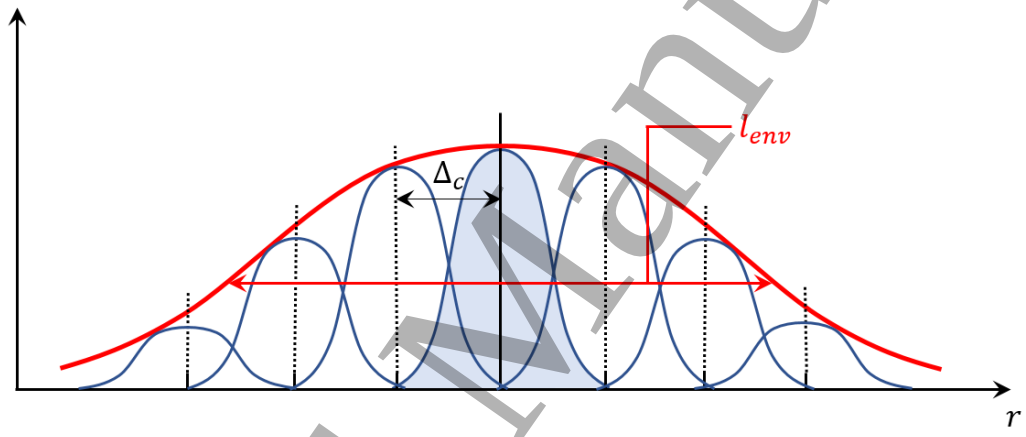

Figure 1. A cartoon about the two radial scales (Δ_c, ℓ_{env}) of the turbulence.

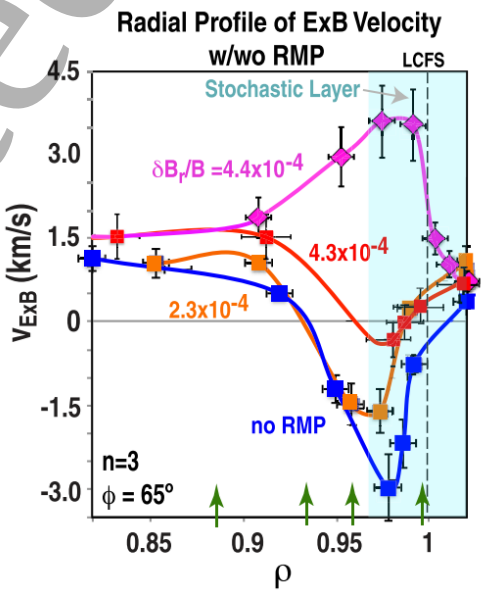

Figure 2. Radial profile of **E**×**B** velocity for cases without and with RMP measured in DIII-D [14].

The most general expression involving the net mean radial current density is actually that for its divergence, i.e.,

$$\frac{\partial\langle J_r\rangle}{\partial r} = \frac{\partial\langle\tilde{V}_r\tilde{\rho}_{pol}\rangle}{\partial r} + \frac{\partial\langle\tilde{b}_r\tilde{J}_\parallel\rangle}{\partial r}. \quad (1)$$

This equation is easily recognized as following from the condition that divergence of the total current vanishes, $\nabla\cdot\mathbf{J}=0$ (i.e., the vorticity equation). The evident counterpart to Eq. (1) is then

$$\langle J_r\rangle = \langle\tilde{V}_r\tilde{\rho}_{pol}\rangle + \langle\tilde{b}_r\tilde{J}_\parallel\rangle. \quad (2)$$

Here, the first term is the flux of polarization charge, and the second is the net flow of current along radially tilted field lines. $\tilde{\rho}_{pol}$ is related to the fluctuation vorticity $\nabla_\perp^2\tilde{\phi}$ with $\tilde{\phi}$ being the fluctuating electrostatic potential, so $\langle\tilde{V}_r\tilde{\rho}_{pol}\rangle$ constitutes the vorticity flux and so contains the Reynolds force via the Taylor identity [48]. The second contribution may be re-written using Ampere's law as

$$\begin{aligned}\langle\tilde{b}_r\tilde{J}_\parallel\rangle &= -\frac{c}{4\pi}\langle\tilde{b}_r\nabla_\perp^2\tilde{A}_\parallel\rangle \\ &= \frac{cB_0}{4\pi}\frac{\partial}{\partial r}\langle\tilde{b}_r\tilde{b}_\theta\rangle. \end{aligned} \quad (3)$$

Here, $\tilde{A}_\parallel$ represents the fluctuating parallel magnetic potential, and B_0 and $\tilde{b}_\theta$ refer to the equilibrium and perturbed poloidal magnetic fields, respectively. The second step in Eq. (3) follows from the Taylor identity. This is explained in Appendix A. Note that the non-ambipolar current density $\langle J_r\rangle$ due to magnetic perturbations is directly proportional to the divergence of the Maxwell stress driven by those perturbations, $\langle J_r\rangle$ is thus determined by both Δ_c scale physics via $\tilde{b}_\theta$, and by ℓ_{env} physics via the divergence of the Maxwell stress. The increment in charge density $\Delta\tilde{\rho}_{pol}$ is then $\partial\langle J_r\rangle/\partial r\sim\partial_r^2\langle\tilde{b}_r\tilde{J}_\parallel\rangle$. Note also that $\int\langle J_r\rangle dr$ vanishes up to boundary contributions, which can, of course, be modified by RMP effects. Thus, there is no net radial current flow, apart from that through the boundary, related to the Maxwell stress exerted there.

To make further progress, one must determine the cross phase between $\tilde{b}_r$ and $\tilde{b}_\theta$.

Here, by $\tilde{b}_r$, $\tilde{b}_\theta$, we refer to magnetic perturbations in the plasma, not the vacuum fields. These, of course, are responsible for local transport in the plasma. To this end, calculations concerning to stochastic magnetic fields are performed in the limit of close proximity to the RMP resonant surface. Note that

$$\langle \tilde{b}_r \tilde{b}_\theta \rangle = -\frac{1}{B_0^2} \sum_k |\tilde{A}_k|^2 \langle k_\theta k_r \rangle, \tag{4}$$

where k_θ and k_r are the poloidal and radial wavenumbers, respectively. Eq. (4) indicates that the radial current density is determined by the spectrally averaged magnetic eddy tilt $\langle k_\theta k_r \rangle$. Now, the evolution of k_r is given by

$$\frac{dk_r}{dt} = -\frac{\partial}{\partial x}(\omega + k_\theta \langle V_E \rangle). \tag{5}$$

Here, ω is the characteristic local frequency of the micro-turbulence, and V_E is the **E**×**B** velocity. Thus, if we ignore $\frac{\partial \omega}{\partial x}$ since $\tilde{b}_k$ is static, it follows that

$$k_r = k_r^0 - k_\theta \langle V_E \rangle' \tau_{ck}. \tag{6}$$

Here, k_r^0 is the initial radial wavenumber of the magnetic perturbations in the plasma, and τ_{ck} is the correlation time for a given mode k. As discussed below, τ_{ck} will be set by scattering and **E**×**B** velocity shear $\langle V_E \rangle'$, and thus is independent of mode frequency. The theory of τ_{ck} is discussed in Appendix B. Then, taking Eq. (6) into Eq. (4), we have

$$\langle \tilde{b}_r \tilde{b}_\theta \rangle = \langle \tilde{b}_r \tilde{b}_\theta \rangle_0 + \frac{1}{B_0^2} \langle V_E \rangle' \sum_{\boldsymbol{k}} \left(|\tilde{A}_k|^2 \, k_\theta^2 \tau_{c,\,b} \right) \tag{7}$$

Here, $\langle \tilde{b}_r \tilde{b}_\theta \rangle_0$ is defined by k_r^0. $\left|\tilde{b}_{r,\,k}^2\right|$ is the intensity of the stochastic magnetic field, and $\tau_{c,\,b}$ is specialized to denote the magnetic correlation time, in order to distinguish it from the potential correlation time shown later. As the L→H transition is approached, we see that $\langle \tilde{b}_r \tilde{b}_\theta \rangle$ becomes proportional to the mean shear $\langle V_E \rangle'$. This is simply the well-known phenomenon of alignment of eddies by shear-induced-tilting, now manifested for externally-induced magnetic fluctuations. Thus, we see that the mean radial current density ultimately is

$$\langle J_r \rangle = \frac{cB_0}{4\pi} \frac{\partial}{\partial r} \left[\langle \tilde{b}_r \tilde{b}_\theta \rangle_0 - \langle V_E \rangle' \sum_{\boldsymbol{k}} \left(\left| \tilde{b}_{r,\,\boldsymbol{k}}^2 \right| \tau_{c,\,b} \right) \right]. \tag{8}$$

The results of Eq. (8) have several notable features. Firstly, Eq. (8) has no explicit dependence upon electron inertia, $\mathbf{k} \cdot \mathbf{B_0}$ resonance, and other familiar elements of test

particle transport by magnetic stochasticity. Of course, this is a consequence of the substitution using Ampere's law to calculate $\langle \tilde{b}_r \tilde{J}_\parallel \rangle$. This result differs dramatically from its often-discussed test particle counterpart, which is the conventional wisdom. At this point, the reader may be wondering about the apparently significant differences between the results in this paper and the well-known quasilinear calculations of [49, 50], and their applications discussed in [51]. This is indeed puzzling since

— the analyses of [49, 50] are in the spirit of a "test particle" calculation, which is quasilinear. Our analysis uses the exact Ampere's law to relate $\tilde{J}_\parallel$ to stochastic fields $\tilde{b}_r$, and entails no linearization. It does not require a further assumption of $\langle J_r \rangle = 0$ to compute the electric field $\langle E_r \rangle$, as in [49, 50]. No ad hoc assumptions regarding viscosity are used, as in [50]. Thus, we submit that this analysis is on a more solid fundamental foundation;

— yet, the analyses of [49, 50] seems to be successful at least at the level of phenomenology reported in [50, 51].

How might one resolve the discrepancy noted above? One promising direction is to note that, as discussed above, $\langle \tilde{b}_r \tilde{J}_\parallel \rangle \sim |\tilde{A}_k|^2 \langle k_\theta k_r \rangle$ with $k_r = k_r^0 - k_\theta \langle V_E \rangle' \tau_{ck}$. Thus k_r^0 is the key. Note that from Ampere's law, we have

$$-\left(k_r^2 + k_\theta^2\right)\tilde{A}_k = \frac{4\pi}{c}\int n_0 |e| v_\parallel \tilde{f}_k d^3v, \tag{9}$$

where $\tilde{f}_k$ is the normalized distribution function. So for $k_r^2 > k_\theta^2$, as applies for RMP, and using the linear response for $\tilde{f}_k$ to $\tilde{A}_k$, we have

$$k_r^2 = -\frac{4\pi n_0 |e|}{c}\int v_\parallel \left(-i\frac{k_\theta}{k}\right)\frac{\delta f_k}{\delta A_k} d^3v. \tag{10}$$

Here, $\frac{\delta f_k}{\delta A_k}$ relates $\tilde{f}_k$, and thus $\tilde{J}_\parallel$, to $\tilde{A}_k$ by the linear response. The latter is fundamental to the test particle quasilinear theory. Solution for k_r will thus link $\langle J_r \rangle$ to $\frac{\delta f_k}{\delta A_k}$ and the test particle result. Of course, magnetic eddy tilting $\widetilde{\boldsymbol{V}}$ will make an additional contribution by $\langle V_E \rangle'$. Observe that the $k_r^0 k_\theta$ contribution appears to capture stochastic field effects on electrons, while the $k_\theta^2 \langle V_E \rangle' \tau_{ck}$ bit is due mainly to ion effects. This competition is the key to the problem. Also, one cannot arbitrarily take $\langle J_r \rangle = 0$, a priori

as in [49, 50]. Rather, one must solve for $\langle E_r \rangle$ from radial force balance in the vein of this paper. Further, detailed analysis is required to elucidate these connections. This will be left to a future work. A key point in this work is the observation that even though $\tilde{b}_r$ is induced by RMP, there still is a physical current fluctuation response in the plasma at the location of $\tilde{b}_r$. So, the local magnetic perturbation still must obey Ampere's law. Hence, we argue that the substitution using Ampere's law gives the correct result. A more challenging calculation is to directly relate $\left|\tilde{b}_r^2\right|$ to the external perturbations. The quasilinear estimate for the diffusion coefficient of stochastic field lines shows a similar proportionality to the strength of stochastic magnetic fields $\left|\tilde{b}_r^2\right|$ [19].

A second feature is the dependence of $\langle J_r \rangle$ upon the magnetic fluctuation envelope structure, i.e., the relation $\langle J_r \rangle \sim \frac{\partial}{\partial r}\left(\left|\tilde{b}_r^2\right|\right)$. This is a consequence of self-consistency and the Taylor identity, which together uncover novel scale dependence on the envelope scale length ℓ_{env}, given by $\ell_{env}^{-1} = \left|\tilde{b}_r^2\right|^{-1} \frac{\partial}{\partial r}\left(\left|\tilde{b}_r^2\right|\right)$. For the application of RMP, ℓ_{env} is quite small with the radial extent being only a few centimeters for the case of DIII-D [14], since the stochastic region is narrowly localized at the edge. Thus, even rather modest levels of $\left|\tilde{b}_r^2\right|$ can produce significant effects near the separatrix, via small ℓ_{env}. This indicates that $\langle J_r \rangle$ is not necessarily "small", even in the absence of electron inertia, etc.

A third related feature is the multi-scale character of the result. Eq. (6) exhibits dependence upon both Δ_c and ℓ_{env}. This is again a consequence of the Ampere's law and the Taylor identity.

In addition to the radial current density $\langle J_r \rangle$, analysis of the L→H transition in the presence of a stochastic magnetic field requires the mean radial *electron* current density $\langle J_{r,e} \rangle$. We can calculate the evolution of mean electron density $\frac{\partial}{\partial t}\langle n_e \rangle$ as

$$\frac{\partial}{\partial t}\langle n_e \rangle = \frac{\partial}{\partial r}\langle \frac{\tilde{b}_r \tilde{J}_{\parallel,e}}{|e|} \rangle = \frac{\partial}{\partial r}\langle \frac{J_{r,e}}{|e|} \rangle. \tag{11}$$

Of course, the fluctuating parallel electron current density requires the elimination of the ion component from the total, i.e., $\tilde{J}_{\parallel,e} = \tilde{J}_{\parallel} - \tilde{J}_{\parallel,i}$, and $\tilde{J}_{\parallel,i} = n_0 |e| \tilde{V}_{\parallel,i}$, where $\tilde{V}_{\parallel,i}$

is the ion flow perturbation. This gives

$$\langle J_{r,e}\rangle = \langle J_r\rangle - n_0|e|\langle \tilde{b}_r \tilde{V}_{\parallel,i}\rangle, \tag{12}$$

where $\langle J_r\rangle$ is given by Eq. (8). Thus, here the net *ion* flow along the tilted lines $\langle \tilde{b}_r \tilde{V}_{\parallel,i}\rangle$ makes an additional contribution. Note that Eq. (12) corrects a trivial sign error in Ref. [52].

$\langle \tilde{b}_r \tilde{V}_{\parallel,i}\rangle$ has been studied intensively in Ref. [52]. Results have been obtained in the limits of $\omega < k_\parallel c_s$ (i.e., static, and stochastic fields, in the presence of weak ambient turbulence) as well as the strong turbulence case $\omega > k_\parallel c_s$. Here, the frequency ω should be taken as referring to both the real frequency and the decorrelation rate, and $k_\parallel$ and c_s represent parallel wavenumber and ion sound velocity, respectively. For the case of $\omega < k_\parallel c_s$ and a pure stochastic field:

$$\langle \tilde{b}_r \tilde{V}_{\parallel,i}\rangle \cong -D_M \frac{\partial\langle V_{\parallel,i}\rangle}{\partial r}, \tag{13-a}$$

where

$$D_M = \sum_{\boldsymbol{k}} |\tilde{b}^2_{r,\boldsymbol{k}}| \pi\delta(k_\parallel), \tag{13-b}$$

is the familiar stochastic field diffusivity and $\langle V_{\parallel,i}\rangle$ is the mean parallel ion flow. Thus,

$$\langle J_{r,e}\rangle = \frac{cB_0}{4\pi|e|}\frac{\partial}{\partial r}\sum_{\boldsymbol{k}}\left[\langle \tilde{b}_r \tilde{b}_\theta\rangle_0 - |\tilde{b}^2_{r,\boldsymbol{k}}|\langle V_E\rangle'\tau_{c,b}\right] + n_0|e|\, D_M \frac{\partial\langle V_{\parallel,i}\rangle}{\partial r}, \tag{13-c}$$

is the net radial electron current density. Similarly, for case of $\omega > k_\parallel c_s$:

$$\langle \tilde{b}_r \tilde{V}_{\parallel,i}\rangle \cong -\frac{1}{\rho c_s^2} D_{st} \frac{\partial\langle P_i\rangle}{\partial r}, \tag{14-a}$$

where

$$D_{st} = c_s^2 |\tilde{b}^2_{r,\boldsymbol{k}}| \tau_{c,b}, \tag{14-b}$$

and ρ and P_i are the ion density and ion pressure, respectively. $\tau_{c,b}$ is particle decorrelation time in the pressure of strong electrostatic turbulence and magnetic stochasticity. Then,

$$\langle J_{r,e}\rangle = \frac{cB_0}{4\pi|e|}\frac{\partial}{\partial r}\sum_{\boldsymbol{k}}\left[\langle \tilde{b}_r \tilde{b}_\theta\rangle_0 - |\tilde{b}^2_{r,\boldsymbol{k}}|\langle V_E\rangle'\tau_{c,b}\right] + n_0|e|\frac{D_{st}}{\rho c_s^2}\frac{\partial\langle P_i\rangle}{\partial r}, \tag{14-c}$$

is the radial electron current density. The $\omega > k_\parallel c_s$ limit is likely the relevant one for the L→H transition, as turbulence intensity increases as the threshold is approached.

Eqs. (13-c) and (14-c) are notable for the additional $\frac{\partial\langle V_{\parallel,i}\rangle}{\partial r}$ and $\frac{\partial\langle P_i\rangle}{\partial r}$ driven contributions to $\langle J_{r,e}\rangle$. These are due to the contribution of ion flow along stochastic magnetic field lines. Notice that in contrast to $\langle J_r\rangle$, the radial electron current density cannot be written as the divergence of a flux. Note that all contributions to $\langle J_{r,e}\rangle$ are proportional to $|\tilde{b}^2_{r,k}|$, with differences resulting from the role of various length scales. In general, $\langle J_{r,e}\rangle$ is driven by magnetic fluctuation intensity gradient as well as by $\frac{\partial\langle V_{\parallel,i}\rangle}{\partial r}$ and $\frac{\partial\langle P_i\rangle}{\partial r}$. $\langle J_r\rangle$ and $\langle J_{r,e}\rangle$ will be used to determine the effect of stochasticity on rotation and transport.

3. Stochastic field effects on poloidal and toroidal rotation

In this section, we examine the effects of stochastic magnetic field induced non-ambipolar transport on mean poloidal and toroidal rotation. These directly enter the mean electric field via radial force balance. The principal impact on $\langle V_\theta\rangle$ and $\langle V_\phi\rangle$ occurs via the mean radial current density $\langle J_r\rangle$ calculated in section 2, through the forces $\langle J_r\rangle B_\phi$ and $\langle J_r\rangle B_\theta$, respectively. For simplicity, we consider the ambient turbulence to be electrostatic.

The poloidal rotation $\langle V_\theta\rangle$ evolves according to

$$\frac{\partial\langle V_\theta\rangle}{\partial t} = -\mu[\langle V_\theta\rangle - \langle V_\theta\rangle_{neo}] - \frac{\partial}{\partial r}\langle\tilde{V}_\theta\tilde{V}_r\rangle - \frac{\langle J_r\rangle B_\phi}{\rho c}. \quad (15)$$

The first term on the RHS of Eq. (15) accounts for relaxation to the neoclassical flow $\langle V_\theta\rangle_{neo}$ at the relaxation rate μ. Here, the expression of neoclassical flow [14, 29] is

$$\langle V_\theta\rangle_{neo} \approx -1.17\frac{\sigma_{neo}}{n_0 e^2}\frac{\partial T_i}{\partial r}, \quad (16\text{-a})$$

and the neoclassical poloidal viscosity

$$\mu = \mu_{00}\left(1 + \frac{\nu_{CX}}{\nu_{ii}}\right)\nu_{ii}. \quad (16\text{-b})$$

Here, σ_{neo} is the neoclassical conductivity, μ_{00} is calculated from the energy weighted momentum equation [53], ν_{CX} and ν_{ii} are the neutral charge exchange (CX) friction

and ion-ion collision frequency, respectively, q is the safety factor, R denotes the major radius. For the second term on the RHS of Eq. (15), it is worth noticing that the Reynolds force and $\mathbf{J} \times \mathbf{B}$ force drive a deviation of shift or the stationary $\langle V_\theta \rangle$ from the neoclassical value $\langle V_\theta \rangle_{neo}$. Here, $\langle J_r \rangle$ has been calculated by Eq. (8). Using this $\langle J_r \rangle$, we can write the stationary poloidal rotation as

$$\langle V_\theta \rangle = \langle V_\theta \rangle_{neo} + \Delta V_\theta, \tag{17-a}$$

where the shift ΔV_θ is

$$\Delta V_\theta = -\frac{1}{\mu}\frac{\partial}{\partial r}\left[\langle \tilde{V}_\theta \tilde{V}_r \rangle - V_A^2 \langle \tilde{b}_r \tilde{b}_\theta \rangle\right]. \tag{17-b}$$

Here, $\langle \tilde{V}_\theta \tilde{V}_r \rangle$ is turbulence driven, while $\tilde{b}_r$ and $\tilde{b}_\theta$ are RMP driven. V_A is the Alfven velocity. Of course, $\langle \tilde{b}_r \tilde{b}_\theta \rangle$ is the magnetic stress due to the stochastic magnetic fields. Taking Eq. (7) into Eq. (17-b), and accounting for alignment of $\tilde{b}_r$ and $\tilde{b}_\theta$ by $\mathbf{E}\times\mathbf{B}$ shear tilting gives

$$\Delta V_\theta = -\frac{1}{\mu}\frac{\partial}{\partial r}\left[\langle \tilde{V}_\theta \tilde{V}_r \rangle - V_A^2 \langle \tilde{b}_r \tilde{b}_\theta \rangle_0 + \langle V_E \rangle' V_A^2 \sum_{\boldsymbol{k}} \left(\left|\tilde{b}_{r,\boldsymbol{k}}^2\right| \tau_{c,b}\right)\right]. \tag{17-c}$$

Note that non-ambipolar transport acts to modify the increment ΔV_θ, and enters via $\frac{\partial}{\partial r}\left(\left|\tilde{b}_r^2\right|\right)$, i.e., the gradient of the stochastic magnetic field intensity. Also, note that ΔV_θ scales inversely with the (large) poloidal flow damping rate μ. Finally, in the likely event (close to transition threshold) that the cross-phase in the Reynolds stress is set primarily by shear induced tilting, we have

$$\Delta V_\theta = \frac{1}{\mu}\frac{\partial}{\partial r}\langle V_E \rangle' \left[\sum_{\boldsymbol{k}} \left|\tilde{V}_{r,\boldsymbol{k}}\right|^2 \tau_{c,\phi} - V_A^2 \left|\tilde{\boldsymbol{b}}_{r,\boldsymbol{k}}^2\right| \tau_{c,b}\right]. \tag{18}$$

In that case, the increments due to the turbulent Reynolds stress and the stochastic magnetic field tend to oppose each other, though they are excited via distinct mechanisms Here, the potential and magnetic correlation times $\tau_{c,\phi}$ and $\tau_{c,b}$ are, in principle, different, but in practice, quite similar. This is due to their common element of $\mathbf{E}\times\mathbf{B}$ shear dependence.

For the case of mean toroidal rotation $\langle V_\phi \rangle$, there are two significant differences with the poloidal rotation. First, neoclassical damping is absent (due to toroidal symmetry) and neoclassical transport is negligible. Second, the Reynolds stress

is now $\langle \tilde{V}_r \tilde{V}_\phi \rangle$. This contains diffusive and residual components, with the former being the most robust. We ignore turbulent residual stress contributions here. Thus, the equation for $\langle V_\phi \rangle$ is

$$\frac{\partial \langle V_\phi \rangle}{\partial t} + \nabla \cdot \langle \tilde{V}_r \tilde{V}_\phi \rangle = \frac{1}{\rho c} \langle J_r \rangle B_\theta + S_\phi. \quad \text{(19-a)}$$

Here, S_ϕ is the external toroidal acceleration. RMP experiments nearly always use toroidal momentum input to drive sufficient rotation to avoid locked modes. Thus, we retain S_ϕ and neglect intrinsic torque. Then using $\langle \tilde{V}_r \tilde{V}_\phi \rangle = -\chi_\phi \frac{\partial}{\partial r} \langle V_\phi \rangle$, where χ_ϕ is the diffusivity of momentum, we have

$$\frac{\partial \langle V_\phi \rangle}{\partial t} - \frac{\partial}{\partial r} \chi_\phi \frac{\partial}{\partial r} \langle V_\phi \rangle = \frac{v_{thi}^2}{\beta} \frac{B_\theta}{B_0} \frac{\partial}{\partial r} \langle \tilde{b}_r \tilde{b}_\theta \rangle + S_\phi, \quad \text{(19-b)}$$

where $\beta = 4\pi P_i / B_0^2$ is the ratio of thermal pressure to magnetic pressure, v_{thi} is the thermal velocity of ions, and we have used Eq. (8) for $\langle J_r \rangle$.

At this point, the reader may indeed be wondering about the residual stress, and its absence from Eq. (19-b). To this end, it is useful to recall that the residual stress is the non-diffusive contribution to the parallel Reynolds stress $\langle \tilde{V}_r \tilde{V}_\phi \rangle$ [54-56], and for electrostatic turbulence, is proportional to $\left\langle k_\theta k_\parallel \left| \tilde{\phi} \right|^2 \right\rangle$. Thus, the residual stress requires spectral symmetry breaking to be non-zero. In practice such symmetry breaking can be due to $\boldsymbol{E} \times \boldsymbol{B}$ shear [57], intensity gradients [58] etc. and enters in proportion to the ratio of scales $X_B / \Delta X_s$ [59]. Here ΔX_s is the spectral width and X_B is the scale associated with symmetry breaking. For examples, in the case of symmetry breaking by $\boldsymbol{E} \times \boldsymbol{B}$ shear, X_B is related to the shift in the spectral structure induced by $\langle V_E \rangle'$. Generally, $X_B / \Delta X_s \ll 1$, so the residual stress is considerably smaller than the diffusive stress. The latter is proportional to χ_ϕ. Intrinsic rotation can still be significant, since the neoclassical damping of toroidal flows is pathetically weak.

The situation becomes is complicated further by magnetic stochasticity, which conflates diffusive scattering of acoustic waves [52, 60] with symmetry breaking. One can estimate that X_B will be 'smeared' over a scale $\delta r \sim (D_M \ell_\parallel)^{1/2}$. Here, D_M is the

magnetic diffusivity [19] and $\ell_\parallel$ is the root-mean-square extent of the spectrum along the field line – i.e. $\ell_\parallel \sim \langle k_\parallel^2 \rangle^{-1/2}$. This smearing due to stochasticity can be expected to reduce $X_B/\Delta X_s$. Thus, we do not consider the residual stress further here. A detailed calculation of the residual stress in the presence of $\langle \tilde{b}_r^2 \rangle$ is quite challenging and must be left to a future work.

Note that magnetic stochasticity effects in Eq. (19-b) seem to be smaller for $\langle V_\phi \rangle$, in proportional to $\frac{B_\theta}{B_0}$. However, since there is no neoclassical damping for toroidal rotation, so $\langle V_\phi \rangle$ is larger ultimately. In the study of mean electric field, it is ultimately the $\mathbf{E} \times \mathbf{B}$ shear $\langle V_E \rangle'$, which is of great interest. The contribution to this due to toroidal rotation is simply proportional to $\langle V_\phi \rangle'$. At steady stage, then, we can obtain the toroidal velocity shear by integrating Eq. (19-b) from the magnetic axis ($r = 0$) to the separatrix $r = r_{sep}$. Taking the shear on the axis as vanishing, we have

$$\frac{\partial}{\partial r}\langle V_\phi \rangle|_{r_{sep}} = -\frac{1}{\chi_\phi}\left[\int_0^{r_{sep}} S_\phi dr + \frac{v_{thi}^2}{\beta}\frac{B_\theta}{B_0}\langle \tilde{b}_r \tilde{b}_\theta \rangle|_{r_{sep}} + C_{sep}\right]. \quad \text{(20-a)}$$

The first term on the right hand side (RHS) is just the net toroidal acceleration, and the second is the weighted Maxwell stress of the stochastic field at the separatrix. The latter is proportional to the total radial current through the separatrix due to magnetic perturbations, i.e.,

$$\int_0^{r_{sep}} \langle J_r \rangle dr = I_{p,r} \sim \int_0^{r_{sep}} \left[\frac{\partial}{\partial r}\langle \tilde{b}_r \tilde{b}_\theta \rangle\right] dr \sim \langle \tilde{b}_r \tilde{b}_\theta \rangle|_{r_{sep}}. \quad \text{(20-b)}$$

The integration constant C_{sep} is set in part, by SOL physics constraints on $\langle V_\phi \rangle'|_{r_{sep}}$. In this regard, some finite 'slip' in $\langle V_\phi \rangle$ can exist at the separatrix, on account of SOL flows and other SOL physics. This possibility of finite slip is usually ignored in the consideration of intrinsic rotation [45, 54, 61, 62]. Eqs. (20-a) and (20-b) tell us that the non-ambipolar current density drives an intrinsic toroidal force, which enters the global toroidal momentum balance. This force may be thought of as due to a flow of current along tilted lines and then ultimately through the separatrix. $\langle J_r \rangle$ then ultimately flows to the divertor plates and interacts with the sheath boundary condition. Finally, we

observe that when shear induced tilting determines the cross correlation in $\langle \tilde{b}_r \tilde{b}_\theta \rangle$, and Eq. (20-a) may be re-written as

$$\frac{\partial}{\partial r}\langle V_\phi \rangle|_{r_{sep}} = -\frac{1}{\chi_\phi}\left[\int_0^{r_{sep}} S_\phi dr + \frac{v_{thi}^2}{\beta}\frac{B_\theta}{B_0}\left[\langle \tilde{b}_r \tilde{b}_\theta \rangle_0 - \langle V_E \rangle' \sum_{\boldsymbol{k}} \left(\left|\tilde{b}_{r,\boldsymbol{k}}^2\right| \tau_{c,b}\right)\right]|_{r_{sep}} + C_{sep}\right]. \tag{21}$$

Eq. (21) gives the toroidal velocity shear at the separatrix induced by magnetic stochasticity.

4. Stochastic field effects on particle and ion heat transport

In this section, we explore stochastic magnetic field effects on transport of particles, i.e. the evolution of mean density and of ion temperature and/or pressure. Particle transport is, of course, also relevant to RMP pump-out [8, 30, 31]. This section is complementary to section 3, in that it elucidates effects on $\frac{\langle \nabla P_i \rangle}{n_i}$, which defines the mean electric field together with $\langle V_\theta \rangle$ and $\langle V_\phi \rangle$ as in the force balance equation.

To calculate how density evolves in the presence of a stochastic layer, we have taken $\langle n_i \rangle = \langle n_e \rangle$ and calculate mean electron density. Proceeding from the continuity equation, we have:

$$\frac{\partial n_e}{\partial t} + \nabla \cdot (n_e \boldsymbol{V_e}) = S_n, \tag{22-a}$$

where the total electron velocity $\boldsymbol{V_e} = \boldsymbol{V}_{\parallel \boldsymbol{e}} + \boldsymbol{V}_{\perp \boldsymbol{e}}$, and S_n is the particle source. Usually, the perpendicular electron velocity $\boldsymbol{V}_{\perp \boldsymbol{e}}$ is due to electrostatic turbulent scattering, while stochastic fields produce wandering of the flow along the parallel direction,

$$\frac{\partial n_e}{\partial t} + \nabla_\perp \cdot (n_e \boldsymbol{V}_{\perp \boldsymbol{e}}) + \nabla_\parallel \cdot (n_e \boldsymbol{V}_{\parallel \boldsymbol{e}}) = S_n. \tag{22-b}$$

Then, retaining only the stochastic field effects, which are the focus here, we have the equation for the mean electron density $\langle n_e \rangle$

$$\frac{\partial n_e}{\partial t} + \frac{\partial}{\partial r}\left[n_0 \langle \tilde{b}_r \tilde{V}_{\parallel,e} \rangle\right] = S_n. \tag{22-c}$$

Now because $\tilde{V}_{\parallel,e} = \tilde{J}_{\parallel,e}/(-n_0|e|)$, in the absence of the particle source term, Eq. (22-c) is simplified to

$$\frac{\partial \langle n_e \rangle}{\partial t} = \frac{1}{|e|}\frac{\partial}{\partial r}\langle J_{r,\mathrm{e}} \rangle. \tag{22-d}$$

Here, $\langle J_{r,\,e}\rangle$ is the mean *electron* radial current density, already calculated in Eqs. (13-c) and (14-c). Recall that $\langle J_{r,\,e}\rangle = \langle J_r\rangle - n_0|e|\langle \tilde{b}_r \tilde{V}_{\parallel,\,i}\rangle$ in Eq. (12), so, for $\omega < k_\parallel c_s$, i.e., weak turbulence,

$$\langle J_{r,\,e}\rangle = \frac{cB_0}{4\pi|e|}\frac{\partial}{\partial r}\langle \tilde{b}_r \tilde{b}_\theta\rangle + D_M n_0 |e| \frac{\partial\langle V_{\parallel,\,i}\rangle}{\partial r}. \tag{23-a}$$

While, for the case of $\omega > k_\parallel c_s$,

$$\langle J_{r,\,e}\rangle = -\frac{cB_0}{4\pi|e|}\frac{\partial}{\partial r}\langle \tilde{b}_r \tilde{b}_\theta\rangle + n_0 |e| \frac{D_{st}}{\rho c_s^2}\frac{\partial\langle P_i\rangle}{\partial r}. \tag{23-c}$$

In the relevant case where the cross phase between $\tilde{b}_r$ and $\tilde{b}_\theta$ is set by electric field shear, as shown in Eq. (7) (i.e., $\langle \tilde{b}_r \tilde{b}_\theta\rangle \approx -\langle V_E\rangle' \sum_k \left(|\tilde{b}_{r,\,k}^2|\tau_{c,\,b}\right)$), the evolution of density is determined by Eqs. (7) and (23).

Integrating Eq. (22-d) gives

$$\frac{\partial N_e}{\partial t} = A_{sep}\frac{1}{|e|}\langle J_{r,\,e}\rangle|_{r_{sep}} + C'_{sep}. \tag{24}$$

Thus, the rate of charge of electron number is simply the radial current through the separatrix. Here, N_e is the total electron number and A_{sep} is the surface area of the plasma at the separatrix. C'_{sep} is an integration constant, set by SOL physics. The result of Eq. (24) also determines the "pump out" caused by RMP induced stochasticity. Here, we add a mild caveat that away from the L→H threshold, the cross phase between $\tilde{b}_r$ and $\tilde{b}_\theta$ is not necessarily set by the mean electric field shear, i.e., $k_r^{(0)}$ is negligible as mentioned above. Mean quasi-neutrality is maintained during pump-out by the ion polarization charge flux, which balances against $\langle J_{r,\,e}\rangle$ to maintain constant net charge. This competition contributes to determining $\langle E_r\rangle$. *We see, too, that the phenomena of RMP induced density pump-out* [50, 63-69] *and the RMP induced increment in the L-H power threshold are deeply linked*. Finally, we see that particle transport is very sensitive to the envelope scale of the magnetic perturbations. From Eqs. (22-d), (23-a) and (23-c), $\frac{\partial\langle n_e\rangle}{\partial t} \sim |\tilde{b}_r^2|/l_{env}^2$. *Thus, a narrow edge stochastic layer can trigger a significant change in density, even for modest magnetic fluctuation intensity* $|\tilde{b}_r^2|$.

Here again, we encounter an apparent puzzle, since $\langle J_r\rangle$ can be computed by

quasilinear theory, and thus used to relate particle density evolution to $\left|\tilde{b}_{r,\boldsymbol{k}}\right|^2$. The condition $\langle J_{r,\mathrm{e}}\rangle \to 0$ then determines the ambipolar potential. The residual flux is an ion flux, but one which is not necessarily small, due to sharp edge intensity gradient. Here, the stress $\langle \tilde{b}_r \tilde{b}_\theta \rangle$, which originates from $\tilde{b}_r \tilde{J}_\parallel$, drives an off-diagonal contribution to the particle flux. An explicit "ion" piece appears in this flux. As discussed above, the k_r^0 contribution to $\langle \tilde{b}_r \tilde{b}_\theta \rangle$ is crucial to reconciling the two approaches. Both approaches ultimately lead to apparently ion driven fluxes. Further, detailed analysis is required, and is left to a future work, as discussed above.

Meanwhile, mean ion pressure evolves according to

$$\frac{\partial \langle P_i \rangle}{\partial t} + \frac{\partial}{\partial r}\langle \tilde{V}_r \tilde{P}_i \rangle = -\rho c_s^2 \frac{\partial}{\partial r}\langle \tilde{b}_r \tilde{V}_{\parallel,i} \rangle. \tag{25}$$

So the principal magnetic effect is due to the divergence of the ion flow along tilted magnetic field lines, i.e., the term on the RHS of Eq. (25). The flux $\langle \tilde{b}_r \tilde{V}_{\parallel,i} \rangle$ was discussed in section 2. Recall that $\langle \tilde{b}_r \tilde{V}_{\parallel,i} \rangle \cong -D_M \frac{\partial \langle V_{\parallel,i} \rangle}{\partial r}$ (Eq. (13-a)) for weak turbulence (i.e., $\omega < k_\parallel c_s$), and $\langle \tilde{b}_r \tilde{V}_{\parallel,i} \rangle \cong -\frac{1}{\rho c_s^2} D_{st} \frac{\partial \langle P_i \rangle}{\partial r}$ (Eq. (14-a)) for strong turbulence(i.e., $\omega > k_\parallel c_s$). Both D_M and D_{st} are defined in Eqs. (13-b) and (14-b), respectively. Note that the characteristic diffusivity is $c_s D_M$ for $\omega < k_\parallel c_s$ and $(\tau_c c_s / l_{ac}) c_s D_M$ (for $\tau_c c_s / l_{ac} < 1$) for $\omega > k_\parallel c_s$, respectively. It is also worthwhile to note that the radial current density $\langle J_r \rangle$ does not enter the determination of $\langle P_i \rangle$. Note too, that $c_s D_M$ is smaller than the thermal ion conductivity, i.e., $c_s D_M < \chi_i$. Thus, for typical cases of drift wave turbulence and values of $\left|\tilde{b}_r^2\right|$, the direct effects of stochasticity on ion heat transport are rather modest. Regarding the effects of magnetic stochasticity on the ion heat transport, this topic was analyzed in [60], and recently in more depth in [52]. The basic physics is simply that ion sound propagation-at speed c_s-sets the fundamental speed for ion heat transport along wandering magnetic field lines. Thus, the effective ion thermal diffusivity is

$$\chi_i = c_s \textstyle\sum_k \left|\tilde{b}_{r,\boldsymbol{k}}\right|^2 \delta(k_\parallel). \tag{26}$$

This should be contrasted to the familiar electron thermal diffusivity of [19]

$$\chi_e = v_{the} \sum_k \left|\tilde{b}_{r,\boldsymbol{k}}\right|^2 \delta(k_\parallel). \quad (27)$$

Obviously, $\chi_i/\chi_e \sim \sqrt{m_e/m_i}$, so $\chi_i \ll \chi_e$ for stochastic field transport. More generally, parallel ion effects are usually the weakest transport channel, due to large ion inertia.

5. Effects of stochastic magnetic fields on turbulence

The bulk of this work is concerned with calculating the mean radial electric field induced by stochastic magnetic fields inside the plasmas. These, in turn, are induced by the plasma response to the external coils. As discussed above, these stochastic magnetic fields in the plasma produce mean field fluxes and stresses, yielding $\langle E_r \rangle$. In addition to all this, the electrostatic turbulence then lives in a background of the stochastic magnetic fields, and thus can differ substantially from its form in the presence of "good flux surfaces". In this section, we review some basic physics of electrostatic turbulence in a stochastic background.

Here, a basic question is one of the scales. For the stochastic field, we expect radially narrow fluctuations, localized to the resonant surface. As k_θ is low due to coils, the magnetic perturbations in the plasma are anisotropic, with $|k_r| > |k_\theta|$. Thus, the ensemble of magnetic perturbations may be viewed as a cluster of current filaments near the rational surface.

The question is then how do these interact with turbulence driven by the heat flux. Note that while ∇T_e driven turbulence and transport will not likely rise above the level induced by the stochastic magnetic field, ∇n_0 and ∇T_i driven modes can likely co-exist with a stochastic background. A question we address is how stochastic magnetic fields modify instability processes and turbulence production. There are old classics on this topic [70-73], in which the effect of stochasticity enters only through electron hyper-resistivity. We have recently developed a more comprehensive theory, with different conclusions. The model analyzes the hydrodynamic theory of the dynamics of a low-k

resistive interchange mode and turbulent relaxation in a high-k (here, $|k|\sim|k_r|$) ambient and static background stochastic magnetic field [74]. Although the mode numbers (either toroidal or poloidal) of the vacuum field generated by RMP coils are small, the plasma response will broaden the spectrum and increase the characteristic mode numbers of this field, especially the radial wave [75]. As illustrated in figure 1, the radial structure of the perturbed magnetic field is very fine, so it is reasonable to assume that the radial wave numbers of $\widetilde{\boldsymbol{b}}$ are large. The choice of resistive interchange treats a generic paradigmatic case, which serves to illustrate the physics of stochastic field effects.

A significant novelty of the theory in [74] is that $\nabla\cdot\boldsymbol{J}=0$ is maintained at *all orders.* As mentioned in section 2, the externally prescribed stochastic magnetic field results in a small-scale current density fluctuation $\tilde{\boldsymbol{J}}_{\parallel}$ along the wandering field. It was shown that $\tilde{\boldsymbol{J}}_{\parallel}$ is not itself divergence free. As suggested in Kadomtsev and Pogutse's classic paper [76] on heat transport in a stochastic field, a temperature fluctuation is generated by the interaction between the mean temperature profile and the imposed magnetic perturbations under the constraint of $\nabla\cdot\boldsymbol{Q_e}=0$, where $\boldsymbol{Q_e}$ is the electron heat flux. The condition $\nabla\cdot\boldsymbol{Q}=0$ significantly constrains the transport flux $\langle\tilde{k}_r\tilde{q}_{\parallel}\rangle$. Here, a small-scale potential fluctuation $\tilde{\varphi}$ must be driven by *the beat of the large-scale test mode and the stochastic field perturbation,* to produce $\tilde{\boldsymbol{J}}_{\perp}$, the fluctuation part of the current density perpendicular to the total field, i.e., a perpendicular current density fluctuation $\tilde{\boldsymbol{J}}_{\perp}$ so as to maintain $\nabla_{\parallel}\widetilde{J_{\parallel}}+\widetilde{\nabla_{\perp}\cdot\boldsymbol{J}_{\perp}}=0$ (see figure 3). This potential fluctuation indicates the presence a spectrum of small-scale convective cells, i.e., electrostatic micro-turbulence produced by stochasticity. Consequently, this theory is intrinsically multi-scale and contains three "players": a large-scale cell, a background stochastic field, and small-scale convective cells (see figure 4) generated by the $\nabla\cdot\boldsymbol{J}=0$ condition. This story departs dramatically from the models based on test particle transport approaches.

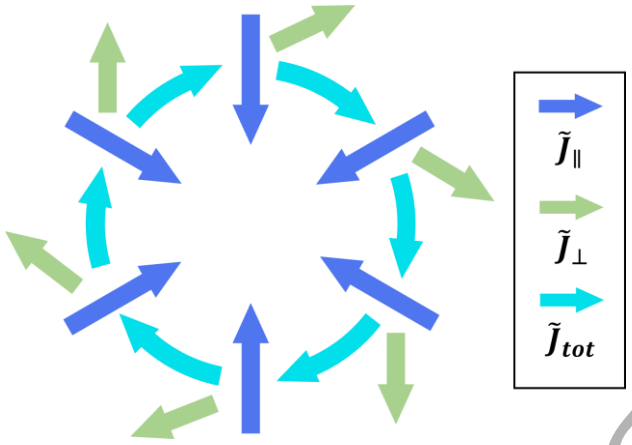

Figure 3. A perpendicular current density fluctuation $\tilde{J}_{\perp}$ is driven to balance $\tilde{J}_{\parallel}$, so that the total current density fluctuation $\tilde{J}_{tot}$ is divergence free. Here, $\tilde{J}_{\parallel}$ and $\tilde{J}_{\perp}$ are fluctuating components of current density parallel and perpendicular to the total magnetic field, respectively [74].

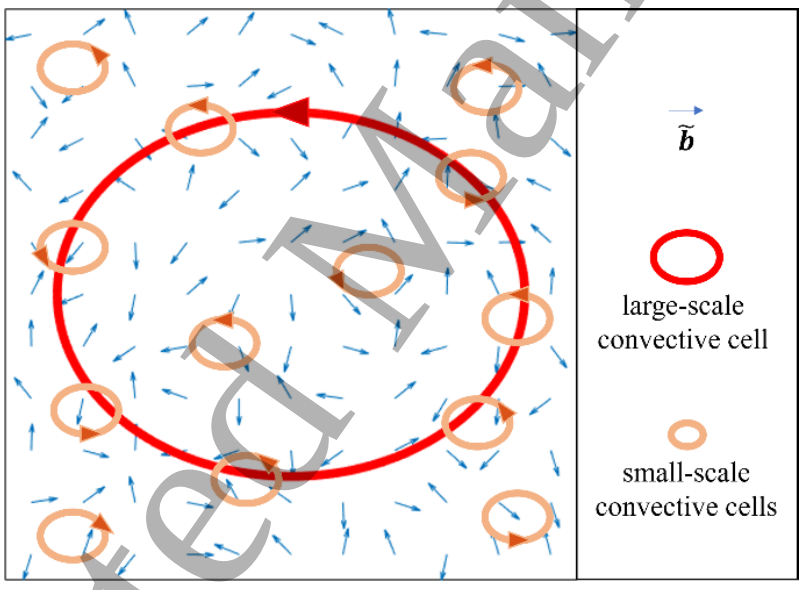

Figure 4. Illustration of the setup of the model in [74].

The stochastic magnetic field converts the eigenmode equation of the test resistive interchange mode to a stochastic differential equation, and introduces a disparity in spatial and temporal scales among the test mode, magnetic perturbations and micro-turbulence. By using method of averaging, the stochastic differential equation is decomposed into two, coupled evolution equations, which describe the large-scale mode and small-scale convective cells, respectively. Macro and micro scales are thus

connected and define a feedback loop, as shown in figure 5.

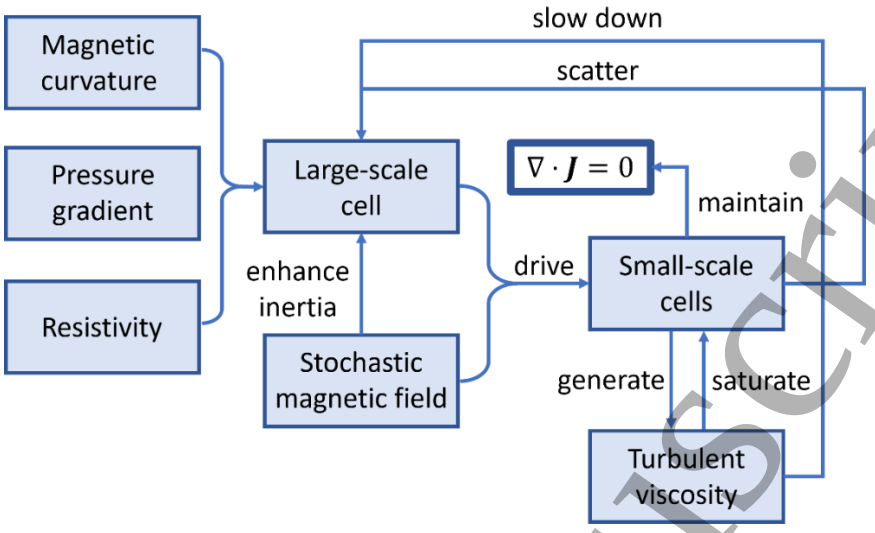

Figure 5. Multi-scale feedback loop of macro and micro-scale interaction of the theory in [74].

Since the model equations in Ref. [74] are complicated, the quantitative description for the mechanism of the drive of micro-turbulence and the connection between macro and micro scales can be reduced to an approximate, simple equation which is similar in form to the Langevin equation, i.e.,

$$\frac{\partial \tilde{\varphi}}{\partial t} + \lambda \tilde{\varphi} = \hat{D}\left[\tilde{b}_r \bar{\varphi}\right]. \tag{28}$$

where λ is the effective friction, and $\hat{D}$ denotes the drive noisey $\tilde{b}_r \bar{\varphi}$ beat. Though the expressions for both λ and $\hat{D}$ are actually complex, Eq. (28) itself indeed reveals part of the physics of our model [74] in a neat manner. It suggests a fluctuation-dissipation balance governs $\tilde{\varphi}$ and shows the dual roles of $\tilde{\boldsymbol{b}}$: on the one hand, $\tilde{\boldsymbol{b}}$ acts as an external noise to excite $\tilde{\varphi}$; on the other hand, micro-turbulence also generates a "turbulent viscosity" which damps these small-scale cells (that's the origin of λ). And in Eq. (28), $\tilde{\varphi}$ and $\tilde{b}_r$ are tightly related, so it is no surprise to find that the correlation $\langle \tilde{b}_r \tilde{v}_r \rangle$ is non-trivial in the model of Ref. [74]. *In other words, the velocity fluctuations "lock on" to the ambient static magnetic perturbations*. In the other half of this feedback loop, micro-turbulence can in turn slow down the growth of the large-scale cell via the

turbulent viscosity and electrostatic scattering. In addition, stochastic magnetic fields can produce a *magnetic braking effect [77]*, which enhances the plasma inertia and opposes the mode growth. This effect may be thoughts of a stochastic analogue of the nonlinear force identified by Rutherford [78]. These effects all tend to oppose the evolution of the fluctuation vorticity. All of these effects can enter how stochastic magnetic fields affect turbulence.

The model of Ref. [74] gives several computationally testable predictions. The appearance of micro-turbulence is consistent with the increase in small-scale structure and spatial roughness, in the turbulence field, as in the simulation of Ref. [79]. The net effect of stochastic magnetic fields is to reduce resistive interchange growth. The increment to the growth rate is calculated by using a perturbation method. The scaling of the turbulent viscosity is calculated via nonlinear closure theory. The correlation $\langle \tilde{b}_r \tilde{v}_r \rangle$ is also calculated explicitly. This correlation can explain the decrease in Jensen-Shannon complexity and predictability observed during the RMP ELM suppression phase on KSTAR [80]. The readers can see [74, 75] for more details.

6. Discussion: Implications for the L→H transition

In this section, we discuss the implications of the results of this paper for the L→H transition. In general terms, there are two types of physical effects induced by stochastic magnetic fields, namely:

i) radial currents and radial flows, i.e., $\langle \tilde{b}_r \tilde{J}_\parallel \rangle$ and $\langle \tilde{b}_r \tilde{V}_{\parallel,\, i} \rangle$, which break ambipolarity. These non-ambipolar transport effects affect the mean radial electric field $\langle E_r \rangle$ via $\langle V_\theta \rangle$, $\langle V_\phi \rangle$ and $\frac{\langle \nabla P_i \rangle}{n_i}$;

ii) scattering by magnetic fluctuations. This tends to dephase $\tilde{V}_r$, $\tilde{V}_\perp$, $\tilde{V}_\parallel$ etc, and thus reduce Reynolds stresses and other transport fluxes. Such enhanced decorrelation processes are discussed at length in Refs. [52, 81, 82].

The primary focus of this paper is on non-ambipolar $\tilde{b}_r$-induced transport effects on $\langle E_r \rangle$. Hence, we summarize the effects of $\langle J_r \rangle$, and related, below. These define an

effective radial Ohm's law ($\langle E_r\rangle \leftrightarrow \langle J_r\rangle$ relation), which is of obvious interest in the context of the L→H transition. In particular, stochastic fields induce a modification in the $\langle V_\theta\rangle$ relative to its neoclassical value calculated in Eq. (17-c) as

$$\Delta V_\theta = -\frac{1}{\mu}\frac{\partial}{\partial r}\left[\langle \tilde{V}_\theta \tilde{V}_r\rangle - V_A^2\langle \tilde{b}_r \tilde{b}_\theta\rangle\right]$$

$$= -\frac{1}{\mu}\frac{\partial}{\partial r}\left[\langle \tilde{V}_\theta \tilde{V}_r\rangle - V_A^2\langle \tilde{b}_r \tilde{b}_\theta\rangle_0 + \langle V_E\rangle' V_A^2 \sum_{\boldsymbol{k}} \left(|\tilde{b}^2_{r,\boldsymbol{k}}|\tau_{c,b}\right)\right],$$

where $\langle V_\theta\rangle = \langle V_\theta\rangle_{neo} + \Delta V_\theta$. Note ΔV_θ is inversely proportional to the neoclassical damping rate μ. Besides, stochastic fields induce a "intrinsic torque" contribution to the toroidal velocity shear at the separatrix that is calculated in Eqs. (20) and (21)

$$\frac{\partial}{\partial r}\langle V_\phi\rangle|_{r_{sep}} = -\frac{1}{\chi_\phi}\left[\int_0^{r_{sep}} S_\phi dr + \frac{v_{thi}^2}{\beta}\frac{B_\theta}{B}\langle \tilde{b}_r \tilde{b}_\theta\rangle|_{r_{sep}} + C_{sep}\right]$$

$$= -\frac{1}{\chi_\phi}\left[\int_0^{r_{sep}} S_\phi dr - + \frac{v_{thi}^2}{\beta}\frac{B_\theta}{B_0}\left[\langle \tilde{b}_r \tilde{b}_\theta\rangle_0 - \langle V_E\rangle' \sum_{\boldsymbol{k}}\left(|\tilde{b}^2_{r,\boldsymbol{k}}|\tau_{c,b}\right)\right]|_{r_{sep}} + C_{sep}\right].$$

Toroidal velocity shear at r_{sep} is modified in proportion to the net non-ambipolar current through the separatrix. Note here that the increment in $\frac{\partial}{\partial r}\langle V_\phi\rangle|_{r_{sep}}$ is inversely proportional to χ_ϕ, so $\Delta\frac{\partial\langle V_\phi\rangle}{\partial r}$ is determined both by stochastic field intensity and by the turbulence intensity. Stochastic fields also affect particle transport via the radial electron current density $\langle J_{r,\mathrm{e}}\rangle$. So the evolution in Eq. (22-d) has been derived

$$\frac{\partial\langle n_e\rangle}{\partial t} = \frac{1}{|e|}\frac{\partial}{\partial r}\langle J_{r,\mathrm{e}}\rangle,$$

where

$$\langle J_{r,e}\rangle = \frac{cB_0}{4\pi|e|}\frac{\partial}{\partial r}\langle \tilde{b}_r \tilde{b}_\theta\rangle - n_0|e|\langle \tilde{b}_r \tilde{V}_{\parallel,i}\rangle.$$

Thus, it shows that $\langle J_{r,\mathrm{e}}\rangle$ necessarily also closely linked to RMP pump-out. Ion heat transport is modified by magnetic effects, albeit rather slightly.

To address the L→H transition, a model is required. Hence, in this paper, we discuss the classes of models and how stochastic magnetic fields affect mean electric field for the L→H transition, as developed in these models. These discussions are relevant to a wide variety of transition models.

Physically, models of the L→H transition may be grouped into three categories or

classes, according to time scales. These are:

i. transport models, describing evolution on transport (in the edge layer) time scales. These models typically are based on transport flux bi-stability. Transport models ignore fluctuation dynamics and time scales, and so can be easily coupled to transport codes;

ii. dynamic models, describing fluctuations, flow shear, etc. These models are typically of the "predator-prey" variety, and involve multiple time scales, but usually address a limited range of spatial scales. Dynamic models are also relevant to drift wave-zonal flow dynamics;

iii. unified models, describing both fluctuation and transport time scale phenomena. Unified models in one spatial dimension describe the build up of the transition, the intermediate phase, and the transition front propagation. Rather few one dimensional (1D) unified models are available.

For transport models, the principal impact of magnetic stochasticity is on toroidal rotation and toroidal velocity shear, via the $\langle J_r \rangle B_\theta$ force. This produces an effective magnetic residual stress. Note that this effect is most pronounced for cases with no momentum input, which are ITER-relevant. Several factors contribute to the sign of $\left(\Delta V_\phi\right)'$, which scales inversely with χ_ϕ, and in proportion to $\frac{B_\theta}{B_0}$, $\langle V_E \rangle'$ and $\left|\tilde{b}_r^2\right|$. We note that few, if any, models have addressed $\langle V_\phi \rangle$ effects on the transition beyond the very simple level of $\mathbf{E}\times\mathbf{B}$ shear-induced-reduction in χ_ϕ. Effects on the particle transport can feedback on transition via $\frac{\langle \nabla P_i \rangle}{n_i}$.

For dynamical models, a key effect is via the evolution of $\langle V_\theta \rangle$ according to:

$$\frac{\partial \langle V_\theta \rangle}{\partial t} = -\mu[\langle V_\theta \rangle - \langle V_\theta \rangle_{neo}] - \frac{\partial}{\partial r}\left[\langle \tilde{V}_\theta \tilde{V}_r \rangle - V_A^2 \langle \tilde{b}_r \tilde{b}_\theta \rangle\right].$$

The fluctuation energy evolution equation would be effectively unchanged from existing models. Obviously, the Reynolds power density $\langle \tilde{V}_\theta \tilde{V}_r \rangle \frac{\partial \langle V_\theta \rangle}{\partial r}$ must conserve energy with its counterpart in the $\langle V_\theta \rangle$ equation. Thus, we see that the principal effects on predator (flow)-prey (fluctuation) models would be the emerging competition

between fluctuation driven Reynolds stress, and the RMP-induced Maxwell stress, which enters via $\langle J_r \rangle B_\phi$. This will lead to an increase in the power threshold required for L→H transition, consistent with experiments. Note that the magnetic intensity profile $\frac{\partial |\tilde{b}_r|^2}{\partial r}$ enters the transition threshold. This introduces a novel scale length ℓ_{env} into the transition problem. Indeed, we speculate that the fast spatial variation in the total Reynolds force introduced by ℓ_{env} will cause the transition to be triggered at the boundary of the stochastic layer, rather than at the outward midplane separatrix, as usual. A study of the dynamical evolution of the transition in 1D, in the presence of an ambient spectrum $|\tilde{b}_r^2|$ suggests itself as an interesting direction for further work. Note that a 1D analysis is essential. This would constitute an interesting step forward for the basic "predator-prey" model.

Unified models will combine all of the aspect discussed above, for transport and dynamic models. Implementing a 1D unified model with ambient $|\tilde{b}_r^2|$ is very challenging and laborious. It is far from certain if a clear trend would emerge. Strong variation with parameters, cases etc. seems likely. We conjecture that the main effects on the power threshold are the "footprint" of the small scale ℓ_{env} and the increase in power threshold due to Reynolds-Maxwell competition. Effects of impurities and energetic particles on the radial electric field are not yet included. There present a conceptual challenge, since one may need to simultaneously satisfy radial force balance for several species. Future work is planned to address this point.

7. Conclusion

In the paper, we presented a mean field theory for **E**×**B** shear in a stochastic magnetic field, such as found in the edge stochastic layer produced by an RMP. Such effects on **E**×**B** shear are of obvious relevance to the L→H transition with RMP, and more generally, in 3D geometry. This paper places special emphasis on the ambipolarity breaking and radial currents. Thus, it defines an effective radial Ohm's Law (i.e. $\langle E_r \rangle \leftrightarrow \langle J_r \rangle$ relation). Complementary studies of dephasing of fluxes, such as for the Reynolds

stress by stochasticity, are published elsewhere. Our study proceeds by exploiting radial force balance to link $\langle E_r \rangle$ to poloidal rotation $\langle V_\theta \rangle$, toroidal rotation $\langle V_\phi \rangle$, electron density $\langle n_e \rangle$ and ion pressure $\langle P_i \rangle$. The effects of stochastic fields, primarily via their induced radial current density, on each of these quantities are elucidated. Their physics is discussed in the context of the L→H transition.

The principal results of this paper are as follows.

i). The radial current density and radial electron current density are calculated from the fundamental flux relation $\langle J_r \rangle = \langle \tilde{b}_r \tilde{J}_\parallel \rangle$, Ampere's law, and the Taylor identity. Then, $\langle J_r \rangle = \frac{cB_0}{4\pi}\frac{\partial}{\partial r}\langle \tilde{b}_r \tilde{b}_\theta \rangle$ gives the non-ambipolar current density generated by $\tilde{b}_r$. Note the proportionality to the Maxwell stress, and that the net radial current vanishes up to boundary contributions, a result in clear contrast with test particle transport models. Note also there is no explicit dependence of $\langle J_r \rangle$ on $\langle E_r \rangle$. The electron current density contains an additional contribution due to ion flow along tilted lines, i.e., $\langle \tilde{b}_r \tilde{V}_{\parallel,\, i} \rangle$;

ii). The phase between $\tilde{b}_r$ and $\tilde{b}_\theta$ is aligned by magnetic eddy tilting, via $\frac{dk_r}{dt} = -\frac{\partial}{\partial x}(k_\theta \langle V_E \rangle)$, so $k_r = k_r^0 - k_\theta \langle V_E \rangle' \tau_{ck}$ as in Eqs. (5) and (6);

iii). The increment of $\langle V_\theta \rangle$ relative to its neoclassical value follows from the **J**×**B** force, and is calculated as $\Delta V_\theta = -\frac{1}{\mu}\frac{\partial}{\partial r}\left[\langle \tilde{V}_\theta \tilde{V}_r \rangle - V_A^2 \langle \tilde{b}_r \tilde{b}_\theta \rangle_0 + \langle V_E \rangle' V_A^2 \sum_{\boldsymbol{k}} \left(\left|\tilde{b}_{r,\,\boldsymbol{k}}^2\right| \tau_{c,\,b}\right)\right]$ in Eq. (17-c). Thus, ΔV_θ scales in proportion to the magnetic perturbation intensity and $\langle V_E \rangle'$ (magnetic eddy tilting alignment) and inversely with poloidal flow damping μ. Of particular note is that the envelope of $\left|\tilde{b}_r^2\right|$ introduces a new, small spatial scale ℓ_{env}.;

iv). The increment in the toroidal velocity shear induced by stochastic magnetic fields also follows from **J** × **B** and is given by $\Delta\left[\frac{\partial}{\partial r}\langle V_\phi \rangle|_{r_{sep}}\right] = \frac{1}{\chi_\phi}\frac{v_{thi}^2}{\beta}\frac{B_\theta}{B_0}\left[\langle \tilde{b}_r \tilde{b}_\theta \rangle_0 - \langle V_E \rangle' \sum_{\boldsymbol{k}} \left(\left|\tilde{b}_{r,\,\boldsymbol{k}}^2\right| \tau_{c,\,b}\right)\right]|_{r_{sep}}$ from Eq. (21). Thus, we see

that $\Delta\left[\frac{\partial}{\partial r}\langle V_\phi\rangle\right]$ at r_{sep} is proportional to the net radial current through the separatrix due to magnetic perturbations;

v). Stochastic RMP driven magnetic fields produce a radial electron current density, which drives particle transport according to $\frac{\partial\langle n_e\rangle}{\partial t} = \frac{1}{|e|}\frac{\partial}{\partial r}\langle J_{r,\mathrm{e}}\rangle$. $\langle J_{r,\mathrm{e}}\rangle$ contains contributions from $\langle J_r\rangle$ discussed above, and from $\langle\tilde{b}_r\tilde{V}_{\parallel,i}\rangle$, which is calculated by Eqs. (13-a) and (14-a). The total electron particle number changes in proportion to the net radial electron current density at the separatrix. Note that this determines the net "RMP pump-out". Indeed, the phenomena of RMP pump-out is closely related to RMP effects on the L→H transition, and radial currents play a key role in each;

vi). Stochastic fields impact ion pressure via the flux $\langle\tilde{b}_r\tilde{V}_{\parallel,i}\rangle$ in Eqs. (13-a) and (14-a). This is related to acoustic-type perturbations, propagating along stochastic field lines. It does not have a simple connection to $\langle J_r\rangle$. Results are given in Eq. (8);

vii). The effects of stochastic magnetic fields on the underlying instabilities and turbulence are summarized in section 3. Stochastic fields induce vorticity braking. More interestingly, we show that non-trivial correlations $\langle\tilde{b}_r\tilde{V}_r\rangle$ develop between the stochastic field and the turbulence. We see that the turbulence tends to "lock on" to the stochastic field.

These results have several implications for the L→H transition. We list them below:

i). First, the stochastic field induced radial current density will tend to compete against the turbulent Reynolds stress, and so will increase the power required to trigger the transition;

ii). The magnetic fluctuation intensity gradient scale is introduced. This can cause transitions to trigger at the boundary of the stochastic layer rather than at the outboard midplane separatrix, as usual;

iii). The stochastic field drives an effective toroidal residual stress, which is the principal effects on the stationary $\langle E_r\rangle$ in H-mode;

iv). The L→H transition power threshold increment with RMP necessarily is linked closely to RMP pump-out, as discussed above. Theory should address both, in a unified and consistent fashion;

v). Detailed modelling is required for quantitative predictions. This is a formidable undertaking. Nevertheless, the results presented in this paper will be useful elements of any model of the L→H transition in a stochastic magnetic field.

A few additional comments are in order here. First, it should be noted that while a seemingly familiar Reynolds stress vs Maxwell stress competition appears, this is not due to Alfvenization since the static magnetic fluctuations $\tilde{b}_r$ are externally driven, while the drift waves are dynamic, and heat flux driven and evolving. Here, the competition is a consequence of eddy tilting by $\langle V_E \rangle'$, which aligns the two. Second, the problem is multi-scale, even in its most simple manifestation. Note that there are five radial scales in the problem, over a highly compressed range, and different orderings are possible. These are summarized in Table 1.

Scale	Physics	Impact
L_n, L_T	Profile gradient	Drive of turbulence
u'/u	Flow damping profile scale	Rotation shear, $\langle V_E \rangle'$
$\ell_{env,\,\phi}$	Drift wave intensity	Reynolds stress drive
$\ell_{env,\,b}$	Stochastic field envelope scale	Magnetic stress scale
k_r	Stochastic field radial wavenumber	Magnetic stress phase

Table 1. Five radial scales in our model, their corresponding physics and impact.

In addition to detailed modelling, several topics remains for future work. These include the consideration of effects on back-transitions and hysteresis. An interesting experiment would be to compare the evolution for RMP switch on and off, and power ramp up and down, performed in different orders. Studies of the effects of ℓ_{env} on the threshold would be of great interest. Modelling of the L→H transition has yet to grapple with the effects of physics related to the edge-SOL connection. These effects naturally couple the transition to the SOL physics and divertor conditions. The connection

becomes especially important when the evolving radial current flows through separatrix. Finally, a deeper understanding of the interplay between radial current and decorrelation effects is required.

Appendix A: $\langle J_r \rangle$ from Taylor identity

As shown in section 2, ambipolarity breaking due to stochastic field will generate the mean current density $\langle J_r \rangle$, and thus affect the rotations and transport. In this appendix, we give a short detail on calculating the $\langle J_r \rangle$ from Taylor identity. $\langle J_r \rangle$ can be calculated from the radial projection of fluctuating parallel current density,

$$\langle J_r \rangle = \langle \vec{J}_\parallel \cdot \vec{e}_r \rangle = \frac{\langle \tilde{J}_\parallel \tilde{B}_r \rangle}{B}, \tag{A1}$$

where $\langle J_\parallel \rangle = \langle J_{\parallel,e} \rangle + \langle J_{\parallel,i} \rangle$. From Ampere law, the fluctuating parallel current density is self-consistent and determined by $\tilde{J}_\parallel = -\frac{c}{4\pi}\nabla^2 \tilde{A}_\parallel$. Thus, we have

$$\begin{aligned}
\langle J_r \rangle &= \frac{\langle \tilde{J}_\parallel \tilde{B}_r \rangle}{B} \\
&= -\frac{c}{4\pi B}\left\langle \frac{\partial}{\partial y}\tilde{A}_\parallel \left(\frac{\partial^2}{\partial x^2} + \frac{\partial^2}{\partial y^2}\right)\tilde{A}_\parallel \right\rangle \\
&= -\frac{c}{4\pi B}\frac{\partial}{\partial x}\left\langle \left(\frac{\partial}{\partial x}\tilde{A}_\parallel\right)\left(\frac{\partial}{\partial y}\tilde{A}_\parallel\right)\right\rangle \\
&= \frac{c}{4\pi B}\frac{\partial}{\partial x}\langle \tilde{B}_x \tilde{B}_y \rangle \\
&= \frac{cB}{4\pi}\frac{\partial}{\partial x}\langle \tilde{b}_x \tilde{b}_y \rangle .
\end{aligned} \tag{A2}$$

Here, x and y correspond to the radial and poloidal directions of tokamak device, respectively. Thus, Eq. (A2) further corresponds to the $\langle \tilde{b}_r \tilde{J}_\parallel \rangle = \frac{cB_0}{4\pi}\frac{\partial}{\partial r}\langle \tilde{b}_r \tilde{b}_\theta \rangle$ as shown in equation (3).

Appendix B: Eddy tilting and correlation time

It is simplest to approach the "eddy tilting", which is relevant to the $\langle k_\theta k_r \rangle$ and further in $\langle \tilde{b}_r \tilde{b}_\theta \rangle$, by working with magnetic potential A. Here A evolves in the presence of mean shear, turbulent scattering and dissipation, so

$$\frac{\partial A}{\partial t} + V_E' \frac{\partial A}{\partial y} + \widetilde{\boldsymbol{V}} \cdot \nabla A = \eta \nabla^2 A. \quad \text{(B1)}$$

Here, we made a local expansion of V_E. Now, turbulent scattering by $\widetilde{\boldsymbol{V}}$ will drive diffusive mixing, so

$$\widetilde{\boldsymbol{V}} \cdot \nabla A = -\frac{\partial}{\partial x} D \frac{\partial}{\partial x} A, \quad \text{(B2-a)}$$

where D is expressed

$$D = \sum_k |\tilde{V}_k|^2 \tau_{ck}. \quad \text{(B2-b)}$$

Hereafter, we drop η. Then, the correlation time for magnetic potential A is set by the familiar process of shear enhanced decorrelation, combining shearing ($\langle V_E \rangle'$) and diffusivity D. Thus,

$$1/\tau_{ck} = (\frac{k_\theta^2 \langle V_E \rangle' D}{3})^{1/3}, \quad \text{(B3)}$$

where k_θ is the azimuthal wave number for $\tilde{b}_r$. Similarly, shear decorrelation will limit the growth of k_r due to tilting, so

$$\frac{dk_r}{dt} \approx -k_\theta \langle V_E \rangle' . \quad \text{(B4)}$$

and thus $k_r = k_r^0 - k_\theta \langle V_E \rangle' \tau_{ck}$ as shown in Eq. (6) in section 2.

Acknowledgements

The authors thank Profs. Xavier Garbet, Lu Wang, Lothar Schmitz, Minjun Choi, George Mckee, Zheng Yan, T. S. Hahm and Yunfeng Liang for many useful discussions. Weixin Guo, Min Jiang, P. H. Diamond and Chang-Chun Chen acknowledge support from the 2019 Festival de Théorie, where this work was initiated. We thank the Festival participants for stimulating interactions. This work was supported by the National MCF energy R&D Program of China under Grant No. 2022YFE03060000, the National Natural Science Foundation of China under Grant Nos. 11905079, 11675059 and 51821005, U.S. Department of Energy, Office of Science, Office of Fusion Energy Sciences, under Award No. DE-FG02–04ER54738 and Award No. DE-SC-0020287, and the Fundamental Research Funds for the Central Universities, HUST: 2019kfyXMBZ034 and 2021XXJS007.

Reference

1. Wagner, F., et al., *Regime of improved confinement and high beta in neutral-beam-heated divertor discharges of the ASDEX tokamak.* Physical Review Letters, 1982. **49**(19): p. 1408-1412.
2. Goldston, R.J., *Energy confinement scaling in Tokamaks: some implications of recent experiments with Ohmic and strong auxiliary heating.* Plasma Physics and Controlled Fusion, 1984. **26**(1A): p. 87-103.
3. Hidalgo, C., *Multi-scale physics and transport barriers in fusion plasmas.* Plasma Physics and Controlled Fusion, 2011. **53**(7): p. 074003.
4. Diamond, P.H., et al., *Dynamics of zonal flow and self-regulating drift-wave turbulence.* 18th IAEA Fusion Energy Conference, Yokohama, Japan, 1998 (International Atomics Energy Agency, Vienna, 1998), 1998: p. IAEA-CN-69/TH3/1.
5. Wilks, T.M., et al., *Development of an integrated core–edge scenario using the super H-mode.* Nuclear Fusion, 2021. **61**(12): p. 126064.
6. Diamond, P.H., et al., *Zonal flows in plasma—a review.* Plasma Physics and Controlled Fusion, 2005. **47**(5): p. R35.
7. Liang, Y., *Overview of edge-localized mode control in tokamak plasmas.* Fusion Science and Technology, 2017. **59**(3): p. 586-601.
8. Evans, T.E., et al., *Suppression of large edge-localized modes in high-confinement DIII-D plasmas with a stochastic magnetic boundary.* Physical Review Letters, 2004. **92**(23): p. 235003.
9. Li, J., et al., *A long-pulse high-confinement plasma regime in the Experimental Advanced Superconducting Tokamak.* Nature Physics, 2013. **9**(12): p. 817-821.
10. Liang, Y., et al., *Magnetic topology changes induced by lower hybrid waves and their profound effect on edge-localized modes in the EAST tokamak.* Physical Review Letters, 2013. **110**(23): p. 235002.
11. Zhang, X., et al., *The factors determining the evolution of edge-localized modes in plasmas driven by lower hybrid currents.* Plasma Physics and Controlled

Fusion, 2020. **62**(12): p. 125013.

12. Zhang, X., et al., *The unstable ELM evolution modulated by lower hybrid waves on EAST.* Plasma Physics and Controlled Fusion, 2020. **62**(9): p. 095007.
13. Yang, Q.Q., et al., *Pace making of edge localized modes with low-hybrid-wave power pulses in the EAST superconducting tokamak.* Plasma Physics and Controlled Fusion, 2019. **61**(6): p. 065023.
14. Schmitz, L., et al., *L–H transition trigger physics in ITER-similar plasmas with applied n = 3 magnetic perturbations.* Nuclear Fusion, 2019. **59**(12): p. 126010.
15. Krommes, J.A., *Plasma transport in stochastic magnetic fields. II: Principles and problems of test electron transport.* Progress of Theoretical Physics Supplement, 1978. **64**: p. 137-149.
16. Diamond, P.H., et al., *Self-Consistent Model of Stochastic Magnetic Fields.* Physical Review Letters, 1980. **45**(7): p. 562-565.
17. Kim, J., et al., *Evolution of magnetic Kubo number of stochastic magnetic fields during the edge pedestal collapse simulation.* Physics of Plasmas, 2018. **25**(8): p. 082306.
18. Fitzpatrick, R., *Helical temperature perturbations associated with tearing modes in tokamak plasmas.* Physics of Plasmas, 1995. **2**(3): p. 825-838.
19. Rechester, A.B. and Rosenbluth M.N., *Electron heat transport in a tokamak with destroyed magnetic surfaces.* Physical Review Letters, 1978. **40**(1): p. 38-41.
20. Krommes, J.A., et al., *Plasma transport in stochastic magnetic fields. Part 3. Kinetics of test particle diffusion.* Journal of Plasma Physics, 1983. **30**(1): p. 11-56.
21. Yu, Q., *Numerical modeling of diffusive heat transport across magnetic islands and local stochastic field.* Physics of Plasmas, 2006. **13**(6): p. 062310.
22. Yu, Q., *Heat diffusion across a local stochastic magnetic field.* Nuclear Fusion, 2007. **47**(9): p. 1244-1249.
23. Hölzl, M., et al., *Numerical modeling of diffusive heat transport across*

magnetic islands and highly stochastic layers. Physics of Plasmas, 2007. **14**(5): p. 052501.

24. Rosenbluth, M.N., et al., *Destruction of magnetic surfaces by magnetic field irregularities.* Nuclear Fusion, 1966. **6**(4): p. 297-300.
25. Tokar, M.Z., et al., *Mechanisms of edge-localized-mode mitigation by external-magnetic-field perturbations.* Physical Review Letters, 2007. **98**(9): p. 095001.
26. Schmitz, O., *Plasma edge transport with stochastic magnetic field structures.* Fusion Science and Technology, 2017. **61**(2T): p. 221-229.
27. Tokar, M.Z., *Stochastic boundary plasmas - basics and applications.* Fusion Science and Technology, 2017. **57**(2T): p. 269-276.
28. Park, G., et al., *Plasma transport in stochastic magnetic field caused by vacuum resonant magnetic perturbations at diverted tokamak edge.* Physics of Plasmas, 2010. **17**(10): p. 102503.
29. Kaveeva, E., et al., *Interpretation of the observed radial electric field inversion in the TUMAN-3M tokamak during MHD activity.* Nuclear Fusion, 2008. **48**(7): p. 075003.
30. Rozhansky, V., et al., *Modification of the edge transport barrier by resonant magnetic perturbations.* Nuclear Fusion, 2010. **50**(3): p. 034005.
31. Paz-Soldan, C., et al., *Observation of a multimode plasma response and its relationship to density pumpout and edge-localized mode suppression.* Physical Review Letters, 2015. **114**(10): p. 105001.
32. Gohil, P., et al., *L–H transition studies on DIII-D to determine H-mode access for operational scenarios in ITER.* Nuclear Fusion, 2011. **51**(10): p. 103020.
33. Kriete, D.M., et al., *Effect of magnetic perturbations on turbulence-flow dynamics at the L-H transition on DIII-D.* Physics of Plasmas, 2020. **27**(6): p. 062507.
34. Kaye, S.M., et al., *L–H threshold studies in NSTX.* Nuclear Fusion, 2011. **51**(11): p. 113019.
35. Ryter, F., et al., *Survey of the H-mode power threshold and transition physics*

studies in ASDEX Upgrade. Nuclear Fusion, 2013. **53**(11): p. 113003.

36. Ryter, F., et al., *L–H transition in the presence of magnetic perturbations in ASDEX Upgrade.* Nuclear Fusion, 2012. **52**(11): p. 114014.
37. Willensdorfer, M., et al., *Dependence of the L–H power threshold on the alignment of external non-axisymmetric magnetic perturbations in ASDEX Upgrade.* Physics of Plasmas, 2022. **29**(3): p. 032506.
38. Scannell, R., et al., *Impact of resonant magnetic perturbations on the L-H transition on MAST.* Plasma Physics and Controlled Fusion, 2015. **57**(7): p. 075013.
39. Kirk, A., et al., *Magnetic perturbation experiments on MAST L- and H-mode plasmas using internal coils.* Plasma Physics and Controlled Fusion, 2011. **53**(6): p. 065011.
40. Leonard, A.W., et al., *Effects of applied error fields on the H-mode power threshold of JFT-2M.* Nuclear Fusion, 1991. **31**(8): p. 1511-1518.
41. In, Y., et al., *Enhanced understanding of non-axisymmetric intrinsic and controlled field impacts in tokamaks.* Nuclear Fusion, 2017. **57**(11): p. 116054.
42. Park, H.K., et al., *Overview of KSTAR research progress and future plans toward ITER and K-DEMO.* Nuclear Fusion, 2019. **59**(11): p. 112020.
43. Xie, P., et al., *Plasma response to resonant magnetic perturbations near rotation zero-crossing in low torque plasmas.* Physics of Plasmas, 2021. **28**(9): p. 092511.
44. Ishizawa, et al., *Multi-scale interactions between turbulence and magnetic islands and parity mixture—a review.* Plasma Physics and Controlled Fusion, 2019. **61**(5): p. 054006.
45. Ida, K. and Rice J.E., *Rotation and momentum transport in tokamaks and helical systems.* Nuclear Fusion, 2014. **54**(4): p. 045001.
46. Peng, S., et al., *Intrinsic parallel rotation drive by electromagnetic ion temperature gradient turbulence.* Nuclear Fusion, 2017. **57**(3): p. 036003.
47. Ding, W.X., et al., *Kinetic stress and intrinsic flow in a toroidal plasma.* Physical Review Letters, 2013. **110**(6): p. 065008.

48. Taylor Geoffrey, I. and William N. Shaw, *I. Eddy motion in the atmosphere.* Philosophical Transactions of the Royal Society of London. Series A, Containing Papers of a Mathematical or Physical Character, 1915. **215**(523-537): p. 1-26.

49. Harvey, R.W., et al., *Electron dynamics associated with stochastic magnetic and ambipolar electric fields.* Physical Review Letters, 1981. **47**(2): p. 102-105.

50. Ashourvan, A., et al., *Role of the edge stochastic layer in density pump-out by resonant magnetic perturbations.* Nuclear Fusion, 2022. **62**(7): p. 076007.

51. Payan, J., et al., *Turbulence during ergodic divertor experiments in Tore Supra.* Nuclear Fusion, 1995. **35**(11): p. 1357-1367.

52. Chen, C.-C., Diamond P.H. and Tobias S.M., *Ion heat and parallel momentum transport by stochastic magnetic fields and turbulence.* Plasma Physics and Controlled Fusion, 2021. **64**(1): p. 015006.

53. Hirshman, S. and Sigmar D., *Neoclassical transport of impurities in tokamak plasmas.* Nuclear Fusion, 1981. **21**(9): p. 1079.

54. Diamond, P.H., et al., *An overview of intrinsic torque and momentum transport bifurcations in toroidal plasmas.* Nuclear Fusion, 2013. **53**(10): p. 104019.

55. Garbet, X., et al., *Turbulence simulations of transport barriers with toroidal velocity.* Physics of Plasmas, 2002. **9**(9): p. 3893-3905.

56. Wang, W.X., et al., *Nonlinear flow generation by electrostatic turbulence in tokamaks.* Physics of Plasmas, 2010. **17**(7): p. 072511.

57. Gürcan, Ö.D., et al., *Intrinsic rotation and electric field shear.* Physics of Plasmas, 2007. **14**(4): p. 042306.

58. Gürcan, Ö.D., et al., *Residual parallel Reynolds stress due to turbulence intensity gradient in tokamak plasmas.* Physics of Plasmas, 2010. **17**(11): p. 112309.

59. Gürcan, Ö.D., et al., *Radial transport of fluctuation energy in a two-field model of drift-wave turbulence.* Physics of Plasmas, 2006. **13**(5): p.052306.

60. Finn, J.M., et al., *Particle transport and rotation damping due to stochastic*

magnetic field lines. Physics of Fluids B: Plasma Physics, 1992. **4**(5): p. 1152-1155.

61. Wang, L. and Diamond P.H., *Gyrokinetic theory of turbulent acceleration of parallel rotation in tokamak plasmas.* Physical Review Letters, 2013. **110**(26): p. 265006.
62. Rice, J.E., *Experimental observations of driven and intrinsic rotation in tokamak plasmas.* Plasma Physics and Controlled Fusion, 2016. **58**(8): p. 083001.
63. Liang, Y., et al., *Active control of type-I edge-localized modes with n=1 perturbation fields in the JET tokamak.* Physical Review Letters, 2007. **98**(26): p. 265004.
64. Evans, T.E., et al., *RMP ELM suppression in DIII-D plasmas with ITER similar shapes and collisionalities.* Nuclear Fusion, 2008. **48**(2): p. 024002.
65. Tamain, P., et al., *Edge turbulence and flows in the presence of resonant magnetic perturbations on MAST.* Plasma Physics and Controlled Fusion, 2010. **52**(7): p. 075017.
66. Wang, S.X., et al., *Investigation of RMP induced density pump-out on EAST.* Nuclear Fusion, 2018. **58**(11): p. 112013.
67. Hu, Q.M., et al., *The density dependence of edge-localized-mode suppression and pump-out by resonant magnetic perturbations in the DIII-D tokamak.* Physics of Plasmas, 2019. **26**(12): p. 120702.
68. Sun, Y., et al., *Nonlinear transition from mitigation to suppression of the edge localized mode with resonant magnetic perturbations in the EAST tokamak.* Physical Review Letters, 2016. **117**(11): p. 115001.
69. Taimourzadeh, S., et al., *Effects of RMP-induced changes of radial electric fields on microturbulence in DIII-D pedestal top.* Nuclear Fusion, 2019. **59**(4): p. 046005.
70. Kaw, P.K., E.J. Valeo, and P.H. Rutherford, *Tearing Modes in a Plasma with Magnetic Braiding.* Physical Review Letters, 1979. **43**(19): p. 1398-1401.

71. Strauss, H.R., *Hyper-resistivity produced by tearing mode turbulence.* The Physics of Fluids, 1986. **29**(11): p. 3668-3671.

72. Bhattacharjee, A. and E. Hameiri, *Self-consistent dynamolike activity in turbulent plasmas.* Physical Review Letters, 1986. **57**(2): p. 206-209.

73. Xu, X.Q., et al., *Nonlinear simulations of peeling-ballooning modes with anomalous electron viscosity and their role in edge localized mode crashes.* Physical Review Letters, 2010. **105**(17): p. 175005.

74. Cao, M. and Diamond P.H., *Instability and turbulent relaxation in a stochastic magnetic field.* Plasma Physics and Controlled Fusion, 2022. **64**(3): p. 035016.

75. Minjun J. Choi, e.a., *Stochastic fluctuation and transport in the edge tokamak plasmas with the resonant magnetic perturbation field.* arXiv:2102.10733v4, 2021.

76. Kadomtsev, B.B. et al., *Electron heat conductivity of the plasma across a'braided' magnetic field.* Plasma Physics and Controlled Nuclear Fusion Research, 1979. **1**: p. 13.

77. Varennes, R., et al., *Synergy of turbulent momentum drive and magnetic braking.* Physical Review Letters, 2022. **128**(25): p. 255002.

78. Rutherford, P.H., *Nonlinear growth of the tearing mode.* The Physics of Fluids, 1973. **16**(11): p. 1903-1908.

79. Beyer, P., Garbet X., and Ghendrih P., *Tokamak turbulence with stochastic field lines.* Physics of Plasmas, 1998. **5**(12): p. 4271-4279.

80. Minjun J. Choi, et al., *Increased fluctuation in the edge tokamak plasmas with the resonant magnetic perturbation field.* arXiv:2102.10733v5, 2021.

81. Chen, C.-C. and Diamond P.H., *Potential vorticity mixing in a tangled magnetic field.* The Astrophysical Journal, 2020. **892**(1): p. 24.

82. Chen, C.-C., et al., *Potential vorticity transport in weakly and strongly magnetized plasmas.* Physics of Plasmas, 2021. **28**(4): p. 042301.